การควบคุมแบบโมเดลพรีดิกทีฟของเซลล์เชื้อเพลิงชนิดเยื่อแลกเปลี่ยนโปรตอน

นางสาวธนาภรณ์ หาเคน

วิทยานิพนธ์นี้เป็นส่วนหนึ่งของการศึกษาตามหลักสูตรปริญญาวิศวกรรมศาสตรมหาบัณฑิต
สาขาวิชาวิศวกรรมเคมี ภาควิชาวิศวกรรมเคมี
คณะวิศวกรรมศาสตร์ จุฬาลงกรณ์มหาวิทยาลัย
ปีการศึกษา 2557

MODEL PREDICTIVE CONTROL OF A POLYMER EXCHANGE MEMBRANE FUEL CELL

Miss Thanaphorn Hakhen

A Thesis Submitted in Partial Fulfillment of the Requirements
for the Degree of Master of Engineering Program in Chemical Engineering
Department of Chemical Engineering
Faculty of Engineering
Chulalongkorn University
Academic Year 2014

Thesis Title	MODEL PREDICTIVE CONTROL OF A POLYMER EXCHANGE MEMBRANE FUEL CELL
By	Miss Thanaphorn Hakhen
Field of Study	Chemical Engineering
Thesis Advisor	Assistant Professor Amornchai Arpornwichanop, D.Eng.

Accepted by the Faculty of Engineering, Chulalongkorn University in Partial Fulfillment of the Requirements for the Master's Degree

.....Dean of the Faculty of Engineering
(Professor Bundhit Eua-arporn, Ph.D.)

THESIS COMMITTEE

.....Chairman
(Associate Professor Anongnat Somwangthanaroj, Ph.D.)
.....Thesis Advisor
(Assistant Professor Amornchai Arpornwichanop, D.Eng.)
.....Examiner
(Associate Professor Soorathep Kheawhom, Ph.D.)
.....External Examiner
(Assistant Professor Yaneeporn Patcharavorachot, D.Eng.)

ธนาภรณ์ หาเคน : การควบคุมแบบโมเดลพรีดิกทีฟของเซลล์เชื้อเพลิงชนิดเยื่อแลกเปลี่ยนโปรตอน (MODEL PREDICTIVE CONTROL OF A POLYMER EXCHANGE MEMBRANE FUEL CELL) อ.ที่ปรึกษาวิทยานิพนธ์หลัก: ผศ. ดร. อมรชัย อาภรณ์วิชานพ, 94 หน้า.

งานวิจัยนี้นำเสนอการประยุกต์ใช้ตัวควบคุมโมเดลพรีดิกทีฟเพื่อควบคุมเซลล์เชื้อเพลิงชนิดเยื่อแลกเปลี่ยนโปรตอน ซึ่งได้พัฒนาแบบจำลองที่มีความไม่เป็นเชิงเส้นของเซลล์เชื้อเพลิงชนิดแลกเปลี่ยนโปรตอนโดยอาศัยสมการสมดุลมวลและพลังงาน ในส่วนแรกของงานวิจัยนี้ศึกษาการหาสภาวะการดำเนินงานที่เหมาะสมที่สภาวะคงตัว ต่อมาศึกษาผลของตัวแปรดำเนินงานที่มีต่อสมรรถนะของพฤติกรรมเซลล์เชื้อเพลิงชนิดเยื่อแลกเปลี่ยนโปรตอนซึ่งมีความสำคัญต่อการออกแบบระบบควบคุม จากการศึกษาตัวแปรต่าง ๆ ที่สภาวะพลวัต พบว่าการเปลี่ยนแปลงของความหนาแน่นกระแส อัตราการไหลของไฮโดรเจนและอากาศขาเข้า และอุณหภูมิของไฮโดรเจนและอากาศขาเข้า ส่งผลต่ออุณหภูมิและค่าความต่างศักย์ไฟฟ้าของเซลล์เชื้อเพลิง นอกจากนี้ได้ออกแบบโครงสร้างการควบคุมเพื่อหาตัวแปรควบคุมและตัวแปรปรับที่เหมาะสมซึ่งจะทำให้ระบบควบคุมมีประสิทธิภาพด้วยการวิเคราะห์อัตราการขยายสัมพัทธ์ จากการศึกษาพบว่าอัตราการไหลเชิงโมลของอากาศและไฮโดรเจนขาเข้าเป็นตัวแปรปรับเพื่อควบคุมอุณหภูมิของเซลล์เชื้อเพลิงและความดันย่อยของไฮโดรเจนตามลำดับ ในส่วนสุดท้ายของงานวิจัยได้นำเสนอการควบคุมโมเดลพรีดิกทีฟแบบที่มีเงื่อนไขบังคับคงทนเชิงออฟไลน์เพื่อควบคุมเซลล์เชื้อเพลิงที่ทำการศึกษาโดยแบบจำลองที่ใช้ถูกจัดให้อยู่ในรูปแบบจำลองเชิงเส้นที่เปลี่ยนแปลงตามเวลาและทำการเปรียบเทียบกับการควบคุมโมเดลพรีดิกทีฟ จากการศึกษาแสดงให้เห็นว่าตัวควบคุมโมเดลพรีดิกทีฟแบบที่มีเงื่อนไขบังคับคงทนเชิงออฟไลน์จะให้สมรรถนะการควบคุมที่ดีกว่าตัวควบคุมโมเดลพรีดิกทีฟ

ภาควิชา วิศวกรรมเคมี ลายมือชื่อนิสิต .....

สาขาวิชา วิศวกรรมเคมี ลายมือชื่อ อ.ที่ปรึกษาหลัก .....

ปีการศึกษา 2557

5470226821 : MAJOR CHEMICAL ENGINEERING
KEYWORDS: POLYMER EXCHANGE MEMBRANE FUEL CELL / CONTROL

THANAPHORN HAKHEN: MODEL PREDICTIVE CONTROL OF A POLYMER EXCHANGE MEMBRANE FUEL CELL. ADVISOR: ASST. PROF. AMORNCHAI ARPORNWICHANOP, D.Eng., 94 pp.

This research presents the application of model predictive control (MPC) to control a proton exchange membrane fuel cell (PEMFC). Firstly, the steady state analysis of PEMFC is considered to select its suitable operating conditions based on cell electrical characteristics. Then, the effect of input parameters on cell voltage and temperature is analyzed to investigate the dynamic behavior of PEMFC that is important for control design. It is found that the cell voltage and cell temperature depend on the inlet molar flow rates and temperature of hydrogen and air, and operating current density. To obtain an efficient control system, the control structure design of the PEMFC is considered to specify a good choice of the controlled and manipulated variables. An analysis of the steady-state relative gain array (RGA) is used for pairing of the controlled and manipulated variables. The result shows that the inlet molar flow rates of hydrogen and air are manipulated variables to regulate the cell temperature and partial pressure of hydrogen, respectively. Finally, a model predictive control (MPC) is developed and designed for controlling the cell temperature and partial pressure of hydrogen. Basically, MPC requires the process model used in its control algorithm. The PEMFC model is known to be complicated and involves uncertain parameters. Thus, an offline robust model predictive control (robust MPC) based on a linear time-varying (LTV) model is proposed for PEMFC control. The simulation results show that the robust MPC shows better control performance than conventional MPC because the robust MPC can guarantee robust stability.

Department: Chemical Engineering Student's Signature .....
Field of Study: Chemical Engineering Advisor's Signature .....
Academic Year: 2014

ACKNOWLEDGEMENTS

This research cannot be perfectly completed without direct and indirect support from several people.

Firstly, I would like to express my appreciation to my thesis advisor, Assistant Professor Amornchai Arpornwichanop for his great support, encouragement, useful suggestions and meticulous corrections throughout the research project.

Moreover, I would like to sincerely thank to the chairman, Associate Professor Anongnat Somwangthanaroj and the other members of the thesis committee, Associate Professor Soorathep Kheawhom and Assistant Professor Yaneeporn Patcharavorachot for their time and useful comments on this thesis.

Next, I would like to acknowledge with much appreciation to my colleague at the Control and Systems Engineering Research Laboratory, Department of Chemical Engineering, and I owe special thanks to Miss Narissara Chatrattanawet, for her suggestion on basic and advanced process control and also helping me finish this project.

Furthermore, I am really appreciated to the Department of Chemical Engineering, Chulalongkorn University for providing the scholarship during my Master's degree study. Financial support by the Ratchadaphiseksomphot Endowment Fund of Chulalongkorn University and the Computational Process Engineering Research Unit is also gratefully acknowledged.

Finally, I truly would like to express my appreciation to my beloved family, especially my mother, Mrs. Suprattra Hakhen, my father, Mr. Warawut Hakhen, and my sister, Miss Benjang Hakhen for the great encouragement, endless love and support.

CONTENTS

Page

Page

Page

LIST OF FIGURE

Page

LIST OF FIGURE

Page

LIST OF TABLE

Page

NOMENCLATURES

A_{act}	Active area (cm^2)
A_i	Vertices in the convex hull
a_c	Parameter for the cathode chemical activity
B_i	Vertices in the convex hull
Co	Convex hull
C_{H^+}	Proton concentration at the cathode membrane/gas interface (mol/cm^3)
C_{H_2}	Liquid phase concentration of hydrogen at anode/gas interface (mol/cm^3)
C_{H_2O}	Water concentration at the cathode membrane/gas interface (mol/cm^3)
c_{p,O_2}	The specific heat of oxygen (J/mol/K)
c_{p,H_2}	The specific heat of hydrogen (J/mol/K)
c_{p,N_2}	The specific heat of nitrogen (J/mol/K)
c^g_{p,H_2O}	The specific heat of gaseous water (J/mol/K)
c^{liq}_{p,H_2O}	The specific heat of liquid water (J/mol/K)
c_{O_2}	Oxygen concentration at cathode/gas interface (mol/cm^3)
c_{H_2}	Hydrogen concentration at anode/gas interface (mol/cm^3)
E	Reversible voltage of the cell (Volt)
E^0	Standard-state reversible voltage (Volt)
F	Faraday constant (C/mol)
G	Non-singular square complex matrix
J	Cost function
j	Operating cell current density (A/cm^2)
j_0	Exchange current density (A/cm^2)
j_{max}	Maximum current density (A/cm^2)
K	State feedback gains

NOMENCLATURES

K_c	Proportional gain
k_{an}, k_{ca}	Mass flow rate coefficients (mol/s.atm)
k_a^o, k_c^o	Intrinsic rate constant for the anode and cathode reactions (cm/s)
ℓ_{mem}	Membrane thickness (cm)
loss L	Loss
M	Control horizon
$\dot{m}$	Molar flow rate (mol/s)
P	Prediction horizon
P_D	Power density (W/m^2)
p_{sat}	Saturation vapor pressure (Pa)
p_{atm}	Ambient pressure (atm)
p_{H_2}, p_{O_2}	Partial pressures of hydrogen and oxygen (atm)
Q	Weighting matrix
R	Gas constant (J/mol/K)
R	Weighting matrix
T	Cell temperature (K)
$T_{\text{air},in}$	Temperature of air (K)
$T_{H_2,in}$	Temperature of hydrogen (K)
T_o	Reference temperature (K)
t	Time (s)
u	Degrees of freedom
V_{cell}	Cell voltage (volt)
V_{act}	Voltage drop due to the activation losses of the anode and cathode (Volt)
V_{ohm}	Ohmic voltage form the resistance of proton though membrane (Volt)
V_{con}	Voltage drop due to the decrease of concentration of the reactants gases (Volt)

NOMENCLATURES

W_{elec}	Electrical work (W)
x	State variable
y	Plant output

GREEK LETTERS

α	Electron transfer coefficient of the reaction at electrodes
ξ	The semi-empirical coefficients
ΔG	Gibbs free energy
ψ	Water content in membrane
η_{real}	Real efficiency
η_{ideal}	Ideal efficiency
η_E	Voltage efficiency
η_F	Fuel utilization efficiency
τ_I	Integral gain
τ_D	Derivative gain
τ_c	Response time constant
τ_1	Time constant
τ_2	Second-order lag time constant
Ω	Polytope for polytopic systems
θ	Time delay
λ_{ij}	Relative gain

SUBSCRIPTS

0	Reference
act	Activation
conc	Concentration

NOMENCLATURES

k	Sampling time
ohm	Ohmic
ss	Steady state condition

CHAPTER I

INTRODUCTION

1.1 Background and Motivation

Rising energy demand and transportation fuelled by petroleum, diesel and natural gas had led to climate change and global warming due to greenhouse gas emissions. Thus, it is required to get rid of or reduce the pollution problems. Recently, a fuel cell has received great attention. It offers the promising alternative to traditional energy conversion technology for applications since it is a power generating device that is high effective in energy conversion, and light weight. It can directly convert chemical energy from fuel into electrical energy. In addition, when the fuel cell engine compares with the internal combustion engine, it can produce electricity with less pollution such as nitrogen oxide (NO_x), sulfur oxide (SO_x), and reduced carbon dioxide (CO_2).

Among the various types of fuel cell, the polymer exchange membrane fuel cell (PEMFC) has attracted considerable interest because of its high energy efficiency, low emission of pollutants to the environment, quick start-up, low-temperature operation (60-100 ^oC) and long life. Therefore, PEMFC is the most attractive candidate for applications in stationary for building and transportation. The material used of the PEMFC is Nafion^{TM}. The significant property of Nafion^{TM} must be high proton conductivity which depends on the level of the humidity of the membrane and vary with its water content, and then fuels are saturated with steam before being supplied to fuel cell at anode in order to keep the hydration of the membrane. For operation of PEMFC, Hydrogen gases that are supplied at the anode divide into hydrogen protons and electrons. The protons transfer through the membrane to the cathode whereas the electrons flow through the external circuit in order to produce electricity. Oxygen in air is supplied to the cathode and associates with the hydrogen ions to produce water and heat as by-product.

The performance of PEMFC depends on many key operating parameters, such as pressure, flow rate and humidity of reactant gases, and temperature (60-100 ^{o}C). For a powerful use of the PEMFC, it is essential to control the hydrogen and air feed, as well as the water produced by the electrochemical reaction. During operation, the feeds of the fuel cell have to be controlled in order to maintain the cell temperature, hydration of the membrane and the reactants in a good level to avoid membrane degradation and to maintain efficiency of PEMFC system (Gruber et al., 2008). Normally, the cell temperature is known to have an importance on transportation within the PEMFC and its performance. When the electrochemical reactions occur and the charges move within the fuel cell stack, heat is released and the fuel cell temperature increases. This improves the rate of the electrochemical reaction and the transport of protons in the membrane, leading to the enhanced PEMFC performance. However, the fuel cell temperature should be limited under a working temperature that does not decompose the material properties of the components. If the fuel cell temperature is too high, the membrane will be damaged. Therefore, the PEMFC performance should be studied.

It is noted that the high fuel cell voltage reveals that the performance of PEMFC is high. On the other hand, the performance of PEMFC is very sensitive to load variations because of low voltage and high current output characteristic of the fuel cell generation system. Thus, a control system becomes importance for PEMFC operation, so as to compensate this effect by making the output voltage as constant as possible. In addition, the interactions of the fuel cell phenomenon such as the thermodynamics, the electrochemical reaction, and the fluid flow make the PEMFC exhibits complex behavior such as high nonlinearity of process with the change in operating point, strong interactions between the variables, and parameter uncertainty, and then control of PEMFC is a challenging task. In the past, there are many researchers have been proposed several methods of control for PEMFC such as feed-forward and feedback control (Pukrushpan et al., 2002; Na et al., 2008), conventional proportional-integral-derivative (PID) (Methekar et al., 2007; S-Y Choe et al., 2008), fuzzy (Hu et al., 2010; Meidanshahi et al., 2012), LQR/LQG strategies (Methekar et al., 2010; A. Niknezhadi et al., 2011), but their performances of these controllers are not sufficient for nonlinear characteristics and parameter uncertainty. To design a smart controller for PEMFC

system that can be implemented, advanced control techniques such as model predictive control (MPC) is interest (Bordons et al., 2006; Gruber et al., 2008; Gruber et al., 2012; Arce et al., 2011). MPC that is model based control strategy is applied to implement the PEMFC system. However, the dynamic model of PEMFC is complex and parameter uncertainty, MPC cannot deal with the uncertain plant model. In order to overcome this limit, the several researchers have been developed the robust model predictive control (robust MPC) for linear time-varying (LTV) system, which handle the problem of robust stability.

In this work, we concentrate on the control of a polymer exchange membrane fuel cell (PEMFC). The transient behaviors of the PEMFC are investigated under various operating parameters. Moreover, control structure design of the PEMFC is considered to specify the good controlled variables and manipulated variables and an analysis of the steady-state relative gain array (RGA) is used for pairing of the controlled and manipulated variables. Finally, the offline robust MPC based on LTV system is implemented to control the PEMFC system and compared with the MPC.

1.2 Objective of Research

The objective of this study is concentrated on the control design of a polymer exchange membrane fuel cell (PEMFC) by using an offline robust MPC algorithm.

1.3 Scope of Research

In this study, the PEMFC fed by pure hydrogen and air is considered. Lumped dynamic model is used, includes mass balances for the anode and cathode side and energy balance for the fuel cell. The transient behaviors of the PEMFC are investigated under various operating conditions. Moreover, control structure design of the PEMFC is considered to specify the good controlled variables and manipulated variables and an analysis of the steady-state relative gain array (RGA) is used for pairing of the controlled and manipulated variables. The performance of the offline robust MPC is evaluated the PEMFC system and compared with the MPC.

1.4 Dissertation overview

Chapter I is an introduction of the research consisting of the importance and reasons for research, the research objectives, the scopes of research and the dissertation overview.

Chapter II gathers the literature reviews on the related studied of the modelling of PEMFC and the control of PEMFC system.

Chapter III provides the basic detail of PEMFC, the procedure of control structure design and the concept of model predictive control model predictive control and robust model predictive control algorithm.

Chapter IV shows the details of dynamic model of a PEMFC including mass balance, energy balance and electrochemical model. Furthermore, the dynamic model is validated against the experimental data and this validated results are revealed. Moreover, the effects of input parameters such as inlet flow rates of hydrogen and air, temperature of hydrogen and air as well as current density on the performance of PEMFC in term of the cell temperature and cell voltage.

Chapter V presents the control structure design of the PEMFC to specify the good controlled variables and manipulated variables and an analysis of the steady-state relative gain array (RGA) is used for pairing of the controlled and manipulated variables. Finally, the offline robust MPC based on LTV system is implemented to control the PEMFC system and compared with the MPC.

Chapter VI shows overall conclusions of the research and recommendations for future research.

CHAPTER II

LITERATURE REVIEWS

This chapter presents the literature reviews for a polymer exchange membrane fuel cell (PEMFC). The reviews concentrate on mathematic model to be suitable for control of PEMFC system. In addition, the control designs of PEMFC are also presented by using many control approaches.

2.1 Modelling of PEMFC

A good PEMFC model can not only help to understand the effect of the design and operating condition but also the internal mechanisms, such as heat and mass transport. In order to improve the performance of PEMFC, it is essential to understand these parameters. There are many literatures for explaining performance on PEMFC by electrochemical models under steady state condition which are described PEMFC characteristics on polarization curve, which related to the voltage and current density. Amphlett et al., (1996) integrated together mechanistic model and empirical relation and proposed a dynamic model of a PEMFC which predicts fuel cell voltage and stack temperature. Moreover, the transportation models are also important for the description of detailed inner-cell. It can be divided three categories, i.e. one dimensional models (1D) (Bernardi and Verbrugge, 1992), two dimensional models (2D) (B. Zhou et al., 2006; J.-H. Jang et al., 2006) and three dimensional models (3D) (M. Hu et al., 2004; Ju et al., 2005; L. Matamoros, D. Bruggemann, 2006; Rismanchi et al., 2008; H.-C. Chiu et al., 2012). These models can be determined the performance of the fuel cell under different steady-state operating conditions and also are used to mathematically describe the electrochemical reaction, the transport phenomena of gases, water, proton and electron and as well as the relationships among fuel cell current, voltage, temperature, and pressure.

While most of the studies have concentrated on steady-state behavior, several papers have recently studied dynamic behavior. For transportation, the PEMFC often

operates under varying load conditions such as during start-up, stop, acceleration and deceleration of electrical vehicles. Therefore, understanding the transient behavior of a PEMFC is benefit for performance control under dynamic loading conditions. Several transient mathematical models of PEMFC (Araki et al., 2005; Baboli and Kermani, 2008; Chang and Chu, 2006, 2007; Real et al., 2007) have been presented including the transport phenomena and thermal dynamics. These models usually require long computation time. Araki et al. (2005) developed a two-dimensional model which considered the mass, charge and energy conservation equations with the equivalent electric-circuit for a PEMFC to obtain distribution of hydrogen/oxygen concentration and current density. Baboli and Kermani (2008) developed a two-dimensional, transient, isothermal and two-phase flow solution to discuss the physics of cathode electrode for PEMFCs.

For PEMFC model to be suitable for control design, it must be low complexity and can predict the dynamic behavior of the system. Yerramalla, Davari et al. (2003) developed a linear and a nonlinear model to consider the humidifier and pressure. Chiu et al. (2004) developed the linear PEMFC models which was used Jacobian linearization via a Taylor series expansion at the nominal operating point. However, control performance perform poor by using the proposed under large disturbances because of the operational parametric uncertainties such as the parametric coefficients for each cell on thermodynamic and electrochemical foundations, and the resistivity of the membrane for the electron flow. Chen et al. (2009) showed a multiple-model approach for a PEMFC system. They used fuzzy clustering to predict characteristic and specified multiple linear models which are altered based on operating condition.

Xue et al. (2004) developed a dynamic model of PEMFC which combines the temperature, gas flow and capacitance effect under operating conditions. The dynamic performance of the cell, the impact of changes in fuel and air inlet temperatures, fuel consumption, and current are studied. The results showed that the gas diffusion will affect the stack temperature which becomes more important when the fuel consumption increases. This model can be implemented in real-time control of PEMFC in automotive and stationary application. Similar work was performed by Pathapati et al. (2005) who proposed a dynamic model to simulate the transient phenomena in PEMFC system. The

analyses show that detailed model of transient effects is necessary and this model can predict PEMFC dynamic behavior under operating conditions.

The control-oriented system-level model is developed (Pukrushpan et al., 2002; Panos et al., 2012; Zhao et al., 2013; Ziogou et al. 2013), it is a better use of the fuel cell capacities and increases the efficiency of the system for control design. This model is combined with principles, empirical relationships and zero-dimensional. Pukrushpan et al. (2002) developed control-oriented fuel cell system model. The transient phenomena includes the flow characteristics, the dynamics of compressor, the main fold filling dynamics and membrane humidity. Simulation result showed that a step change in current requires, oxygen excess ratio drops due to depletion of oxygen. This causes the stack voltage drop. In addition, the model results were reasonable with the experiment results. But they do not considered temperature variation. A simple empirical model was proposed by del Real et al. (2007) to develop the fuel cell voltage with the main variable variations.

Hu et al. (2010) presented a dynamic mathematical model including a coolant circuit model based on the model conservation and energy balance theory. They simulated the dynamic characteristics of the PEMFC coolant circuit under the several load current steps input.

Panos et al. (2012) developed the dynamic mathematical model includes mass balances for the anode and cathode side, recirculation, semi-empirical equations for the membrane, electrochemical equations, heat balances for the fuel cell and mass and energy equation for the humidifier, compressor and the cooling system.

Zhao et al. (2013) used a dynamic model for PEMFC system optimization and control. They studied dynamic behavior of PEMFC associated with the reactant flow, cooling water flow, and water phase change.

Ziogou et al. (2013) developed a dynamic mathematical model that takes into account main variables and parameters, such as, the partial pressures of gases, the operating temperature and the cell current. This model is used for the formulation of the model-based controller of the PEMFC system.

2.2 Control of PEMFC

A PEMFC is a nonlinear, multi-input and multi-output (MIMO) system. Therefore, to obtain a reliable and efficient response and prevent degradation of membrane, it is essential to design control scheme to achieve optimal hydrogen and air flow rates. Controller designs can be produced by using smart control approaches such as feed-forward and feedback control (Pukrushpan et al., 2002; Na et al., 2008), PID (Methekar et al., 2007; S-Y Choe et al., 2008), fuzzy (Hu et al., 2010; Meidanshahi et al., 2012), LQR/LQG strategies (Methekar et al., 2010; A. Niknezhadi et al., 2011), and model predictive control (MPC) (Bordons et al., 2006; Gruber et al., 2008; Gruber et al., 2012; Arce et al., 2011). Several control approaches have been proposed in the literature and configurations can be used for controlling the PEMFC system.

Pukrushpan et al. (2002) developed three major control subsystems such as air/fuel supply, heat management and water management in PEMFC. They combined feedforward and feedback controller to regulate the excess oxygen ratio in the cathode during step changes in current demand and achieve the desired net power of PEMFC. Na et al. (2008) proposed a dynamic nonlinear model for the PEMFCs and designed a nonlinear control by feedback linearization in order to regulate the derivation of hydrogen and oxygen pressure during load variation. Control inputs are the inlet flow rates of hydrogen and air. However, the proposed nonlinear controller cannot guarantee the robustness with the operational parametric uncertainties. Therefore, advanced controller designs need to be developed, considering the nonlinearity and uncertainty plant that need to be studied.

In addition, a variety of control strategies have been proposed PID controller and their control configurations can be utilized for control the PEMFC performance. Three components of PID are proportional (P), integral (I), and derivative (D). P controller makes the offset so integral action eliminates the offset but resulting oscillation. Temperature control strategy based on a thermal circuit was proposed by S-Y Choe et al. (2008). A classical PI controller and state feedback controller for the thermal circuit were used in control design. The results show that the proposed control strategy cannot suppress a temperature increase in the catalyst layer.

Methekar et al. (2007) considered a multi-input and multi-output (MIMO) system where average power density and average solid temperature are the two controlled outputs. Moreover, they studied many manipulated variables such as the inlet molar flow rate of O_2 and H_2, the inlet gas temperature of anode and the cathode, and the inlet molar flow rate of coolant. They employed IMC based PI controllers for the power control loop and temperature loop using a cascade control scheme. However, this multi-loop approach cannot handle nonlinear and multivariable interactions.

Other approaches proposed advanced control strategies for PEMFC such as a model predictive control (MPC). The basic concept of MPC design is to predict the future plant response of a process model and usually trying to minimize a finite horizon objective function which consists of a sum of future predicted errors and control moves. In MPC, each step is taken while new changes in disturbance and the desire values are considered. Advantage of MPC is capable to deal with nonlinear processes, multivariable interactions, and input constraints. Vahidi et al. (2006) used a model predictive control strategy to avoid starvation and simultaneously match an arbitrary level of current demand. They studied the starvation problem in a hybrid fuel cell system.

A multiple-model predictive controller for a hybrid PEMFC system was considered by Chen et al. (2009). In multiple-model MPC design, an upper-layer adaptive switch is added that determines the models should be used within each sampling period. However, the implementation can be computationally expensive and switching between linearized models can cause perturbations.

Wu et al. (2009) implemented a multi-loop nonlinear predictive control. Both oxygen excess ratio and stack temperature of a hybrid energy system are the controlled variables by manipulating air (oxygen) and coolant flow rate. The loop interactions of PEMFC system are analyzed for choosing controlled and manipulated variables by step changes in the inputs. However, it does not guarantee the system stability.

Methekar et al. (2010) proposed an approach based on the identification of state space models, and used these models for developing LMPC control schemes for the

PEMFC. They studied the problem of controlling average power density and average solid temperature in a PEMFC by manipulating hydrogen and coolant flow rates.

Gruber et al. (2009) experimentally designed a constrained MPC for the air feed fuel cell to control the oxygen excess ratio using the compressor motor voltage to manipulate the air flow rate. Recently, Gruber et al. (2012) experimentally proposed NMPC strategy based on a second order Volterra series model in order to regulate the oxygen excess ratio by using the compressor motor voltage as control input. The results showed that the proposed NMPC cannot be durable after changes in the current, the PEMFC system exhibit a faster transient behavior.

Ziogou et al. (2013) considered dynamic model and developed NMPC controller to avoided oxygen starvation and minimize hydrogen consumption by manipulating the air and hydrogen flows. It is demonstrated that the system can modify to set-point changes of the load demand under varying conditions. However, NMPC does not guarantee closed-loop stability.

Although MPC is able to handle operational constraints of the system during the design of the control loop, a lot of issues still need to be studied. Especially, MPC robustness is the critical point when model is uncertain. Model uncertainty remains in MPC because there are differences between the model used for prediction and the real dynamics of the plant to be controlled. Then the performance of the control loop performs poorly and the optimization problem may become unfeasible. Hence, Robust Model Predictive Control was proposed by Kothare et al., 1996 is attention. Since it can guarantee the robust stability of the closed loop system by minimizing an upper bound on the worst-case objective function subject to input and output constraints over Linear Matrix Inequality (LMI)

CHAPTER III

THEORY

3.1 Fuel Cell

A fuel cell is an electrochemical device that converts the chemical energy of reaction of fuel with an oxidant into the electrical energy. The only by-products of the electrochemical reaction in a fuel cell are heat and water without combustion fuel and pollution. The reaction can be expressed as follow:

$$H_2 + \frac{1}{2}O_2 \rightarrow H_2O \tag{3.1}$$

The advantages of fuel cells are several compared to the conventional systems that produce electricity such as high efficiency, quiet operation, environmentally friendly, flexibility of fuel and high energy density. Consequently, the fuel cells are attractive energy technologies of the future. Fuel cells are classified by type of electrolyte they use. This can be divided by the electrochemical reactions, the catalysts requirement, the temperature ranges, and other parameters. There are five major types of fuel cells, based on the type of the electrolyte used: Polymer exchange membrane fuel cell (PEMFC), Alkaline fuel cell (AFC), Phosphoric acid fuel cell (PAFC), Molten carbonate fuel cell (MCFC), Solid oxide fuel cell (SOFC). The summary of each type of fuel cells are shown in Table 3.1

3.2 Polymer Exchange Membrane Fuel Cell (PEMFC)

The polymer exchange membrane fuel cell (PEMFC), also known as polymer exchange membrane fuel cells, is the most attractive for automobiles and small stationary applications due to its high power density, low operating temperatures (around 60-100 °C), fast start-up, and zero emission.

Table 3.1 The summary of each type of fuel cells

Type	Electrolyte	Operating Temperature (C)	Efficiency	Power density (kW/m2)
PEMFC	Polymer membrane	60-100	35-55%	3.5-13.5
DMFC	Polymer membrane	50-100	40-50%	1.0-6.0
AFC	Potassium Hydroxide	50-200	45-60%	0.7-8.1
PAFC	Phosphoric Acid	160-210	40-50%	0.8-1.9
SOFC	Ceramic	500-1000	50-65%	1.5-5.0

3.2.1 Parts of a PEMFC

The key structure of a typical PEMFC which consists of seven components: flow channel, gas diffusion layer (GDL), and catalytic layer in the anode; membrane; catalytic layer, gas diffusion layer (GDL), and flow channel in the cathode are presented in Figure 3.1

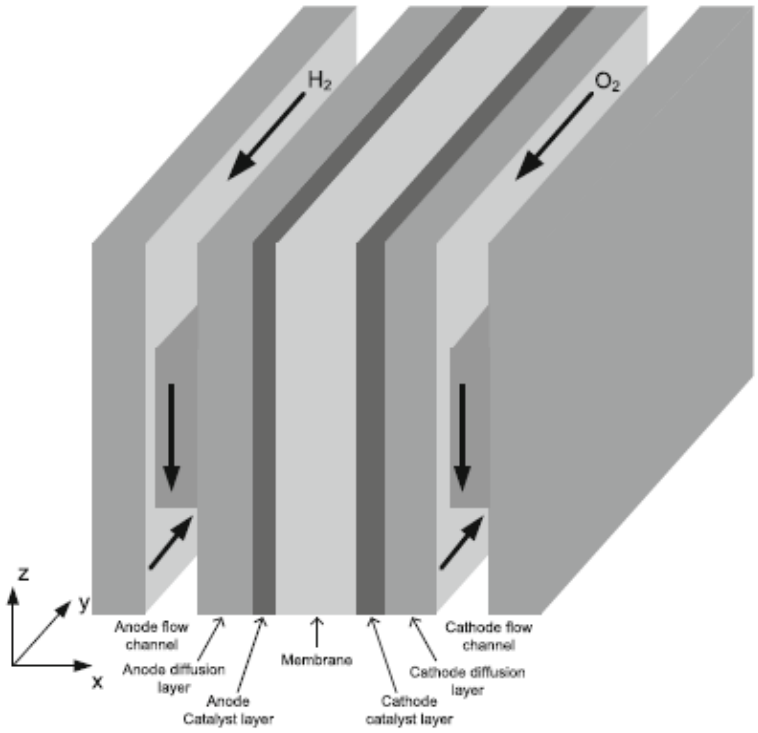

Figure 3.1 The structure of a PEMFC (Feroldi and Basualdo 2012)

As shown in Figure 3.1, the membrane electrode assembly (MEA) is the heart of a PEMFC. The MEA consists of a membrane, two catalyst layers, and two gas diffusion layer (GDL) which are fabricated and pressed together. The MEA is the critical interface between the membrane and the electrodes since it is the site of the reaction of a PEMFC.

3.2.2 The Operation of a PEMFC

A PEMFC converts the chemical energy of a fuel and an oxidizer into electrical energy. The anode is left side of a single cell; the fuel or hydrogen is supplied through an anode and the cathode is right side of a single cell; the oxidizer or oxygen in air is supplied at cathode. Figure 3.2 display transport phenomena of gases, protons, and electrons in a PEMFC electrode. The mechanism can be shown step by step as below:

Hydrogen flows through gas channels on anode side of a fuel cell. It diffuses through diffusion layers to the catalytic layer where it oxidizes to form proton and electrons, as shown below in the reaction:

$$H_2 \rightarrow 2H^+ + 2e^- \tag{3.2}$$

Proton ions are transferred through the membrane, which is an insulator for electrons to the catalytic layer of cathode. Electrons pass through current collector and external electric circuit to cathode. On cathode side of a fuel cell, the oxygen or air is consumed with protons ions and electrons to form water:

$$2H^+ + 2e^- + \frac{1}{2}O_2 \rightarrow H_2O \tag{3.3}$$

Then overall chemical reaction occurring inside PEMFC is

$$H_2 + \frac{1}{2}O_2 \rightarrow H_2O \tag{3.4}$$

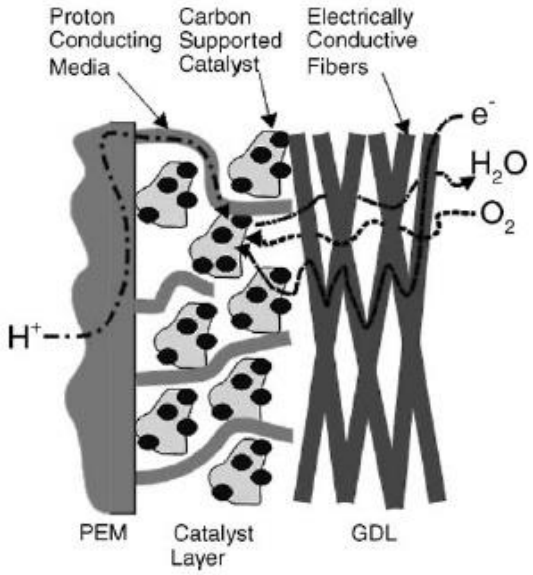

Figure 3.2 Transport phenomena of gases, protons, and electrons in a PEMFC electrode (Litster and McLean 2004)

3.2.3 PEMFC Performance

3.2.3.1 Thermodynamics of PEMFC

Thermodynamics is the study of energy changing from one stage to another. The conversion of the free energy change associated with a chemical reaction directly into electrical energy is the electrochemical energy conversion. Maximum electrical work (W_{elec}) is given by the negative change in Gibbs free energy change (ΔG) for the process, and can be expressed in molar quantities as:

$$W_{elec} = -\Delta G \tag{3.5}$$

The potential of a system to perform electrical work by a charge, Q (coulombs), through an electrical potential difference, E (Volts), is

$$W_{elec} = EQ \tag{3.6}$$

If the charge is assumed to be carried out by electrons:

$$Q = nF \tag{3.7}$$

where n is the number of moles of electrons transferred and F is the Faraday's constant (96,487 coulombs per mole of electrons). Therefore, the maximum reversible voltage can be provided by the cell as in Eq. (3.8),

$$\Delta G = -nFE_r \tag{3.8}$$

where E_r is the standard reversible potential.

For any chemical reaction

$$aA + bB \rightarrow cC + dD \tag{3.9}$$

The Gibbs free energy can be expressed in terms of the standard state Gibbs free energy and the partial pressures of the reactants and products:

$$\Delta G = \Delta G^{O} + RT\ln\frac{\left(p_c/P_0\right)^c\left(p_D/P_0\right)^d}{\left(p_A/P_0\right)^a\left(p_B/P_0\right)^b} \tag{3.10}$$

The overall reaction is the oxidation of H_2 to form H_2O, namely,

$$H_2 + \frac{1}{2}O_2 \rightarrow H_2O \tag{3.11}$$

In this reaction, the number of moles of electrons transferred for one mole of reacted hydrogen is 2 (n=2) and then,

$$E = -\frac{\Delta G}{nF} = -\frac{\Delta G^0}{nF} - \frac{RT}{nF}\ln\left(\frac{p_{H_2O}}{p_{H_2}p_{O_2}^{1/2}}\right) \tag{3.12}$$

$$E = E^0 - \frac{RT}{2F}\ln\left(\frac{p_{H_2O}}{p_{H_2}p_{O_2}^{1/2}}\right) \tag{3.13}$$

Eq. (3.13) can be called Nernst Equation; it depends on the gas composition and temperature at the electrodes. E is the open circuit voltage, E^0 is the standard-state reversible potential, R is the gas constant, and T is the cell temperature.

3.2.3.2 Actual performance

The electrical energy is obtained from a fuel cell only when a current is drawn. However, the actual fuel cell voltage (V_{cell}) is less than the open circuit voltage (E^{OCV}) because of the various irreversible losses (V_{loss}). These losses are referred to as

polarization: activation polarization (V_{act}), ohmic polarization (V_{ohmic}), and concentration polarization (V_{conc}). Figure 3.3 shows the different regions and the polarization effects (triangle dot). There are three divided field in fuel cell performance curve: at low current density, in region (A), the cell voltage is influenced by the electrochemical reaction which is called activation losses. At high current density, the cell voltage is decreased due to the resistance of the fuel cell in region (B), which is called ohmic losses. In region (C), the reduction in concentration reactants which causes the cell voltage breaks down. It is called concentration losses (Shen, Meuleman et al. 2003). In general, the actual fuel cell potential (V_{cell}) is defined as:

$$V_{cell} = E^{OCV} - V_{act} - V_{ohm} - V_{conc} \tag{3.14}$$

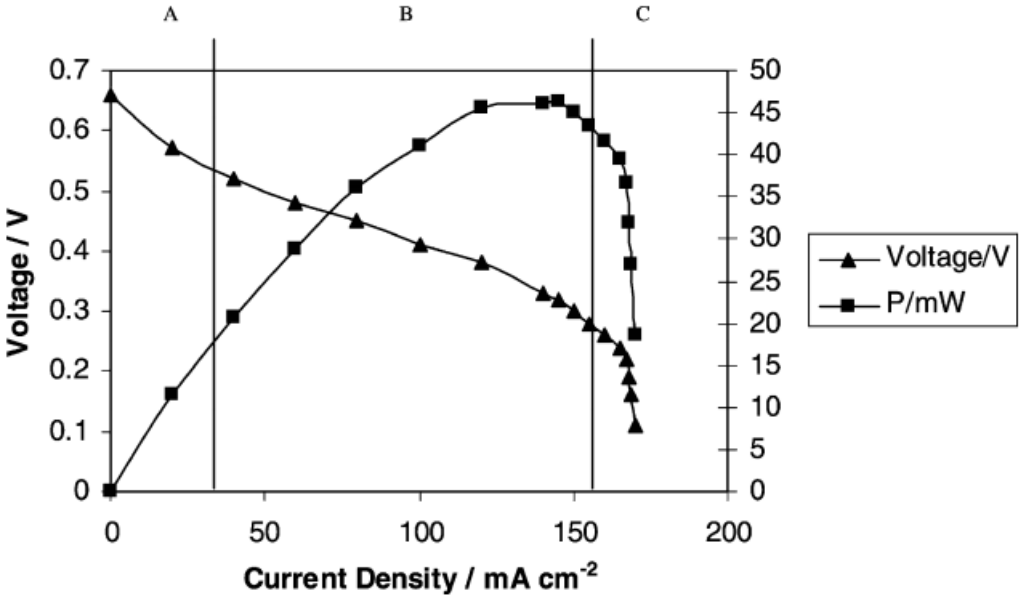

Figure 3.3 Performance curve of a PEMFC (Shen, Meuleman et al. 2003)

3.2.3.2.1 Activation Polarization (V_{act})

The activation polarization is the voltage loss, which caused by the slowness rate of the electrochemical reaction taking place on the electrodes surface. In a PEMFC, the activation polarization at the anode side is smaller than the cathode side because the exchange current density of the anode reaction is higher than that of the cathode

reaction, so this loss at the anode side is omitted. In the most case, the activation polarization can be described by the Tafel equation

$$V_{act} = \frac{RT}{\alpha nF} \ln \frac{j}{j_0} \tag{3.15}$$

where α is the electron transfer coefficient of the reaction at electrodes, j is current density (A/cm^2), and j_0 is the exchange current density (A/cm^2).

3.2.3.2.2 Ohmic Polarization (V_{ohmic})

The ohmic polarization is the voltage losses from resistance of ions flowing pass the electrolyte, the resistance of electrons flowing pass the electrodes, and the resistance of fuel cell components. The ohmic losses can be expressed using general equation of Ohm's law as following:

$$V_{ohm} = IR_{ohmic} \tag{3.16}$$

where R_{ohmic} is the total internal cell resistance, which includes electron, proton and membrane. I is the cell current (A).

3.2.3.2.3 Concentration Polarization (V_{conc})

The concentration polarization or mass transport polarization is the losses due to the reduction in concentration reactants at the electrodes surface as the hydrogen is consumed. The concentrations of the hydrogen and air are decreased at the various points in the channel and are less than the concentrations at the inlet value of the stack. At higher currents density when the hydrogen and air are used at higher rates and the concentration in the channel is decreased. The concentration loss can be represented by the following equation

$$V_{conc} = -B\ln(1-\frac{j}{j_{\max}}) \tag{3.17}$$

where j_{max} denotes the maximum current density (A/cm^2) and B is the constant value, which depends on the cell and its operating state.

3.2.3.3 Power Characteristic

In a PEMFC, the power density (P_D) is a product of voltage and current density and expressed as follow:

$$P_D = V_{cell} jA_{act} \tag{3.18}$$

Figure 3.3 also represents the power density characteristic curve for PEMFC (square dot). The peak power density is called the maximum power density and is used to determine the performance of a PEMFC. It should select the desire operating condition range according to high power are required for application.

3.2.3.4 Fuel Cell Efficiency

The real efficiency of fuel cell can be expressed into:

$$\eta_{real} = \eta_{ideal}\eta_E\eta_F \tag{3.19}$$

3.2.3.4.1 Ideal Efficiency

The efficiency (η) is the amount of useful energy that can be obtained from the process to the total energy expressed by following equation:

$$\eta = \frac{useful\ energy}{total\ energy} \tag{3.20}$$

For a fuel cell, the maximum energy produced by the fuel cell is equal to the maximum charge of Gibbs free energy of formation. Therefore, the reversible energy efficiency of fuel cell can be expressed as:

$$\eta_{ideal} = \frac{\Delta G}{\Delta H} \tag{3.21}$$

3.2.3.4.2 Voltage Efficiency

The voltage efficiency of fuel cell is the ratio of the real operating voltage (V_{cell}) of the fuel cell to the reversible voltage of the fuel cell (E^{OCV}):

$$\eta_E = \frac{V_{cell}}{E^{OCV}} \tag{3.22}$$

3.2.3.4.3 Fuel Utilization Efficiency

The fuel utilization efficiency is defined by the ratio of fuel used by the cell to generate electric current versus the total fuel provided to the cell.

$$\eta_F = \frac{I / nF}{m_{fuel}} \tag{3.23}$$

where m_{fuel} is the mole flow rate at which fuel is supplied to the fuel cell (mol/sec)

3.3 Control Structure Design

This section, the selection of the good controlled variables is considered. The aim is to study the selection of the controlled variables of the system by finding a self-optimizing control structure for the controlled variables keep them constant at their set-points and leads to near optimal operation when disturbances appear within the system.

Self-optimizing control is to control structure approach can achieve an acceptable loss with constant set-point values for the controlled variables without the re-optimization when disturbances appear within the system. (Skogestad 2004)

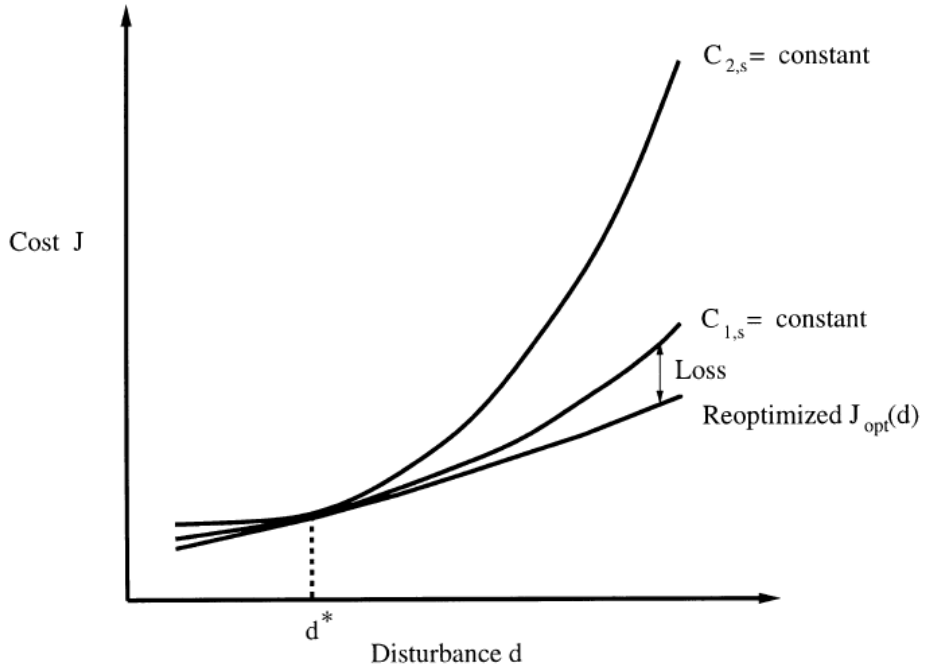

Figure 3.4 Loss imposed by keeping constant set-point for the controlled variable (Skogestad 2004)

Figure 3.4 displays that when the disturbance move away from its nominal optimal operating point, there is a loss when we need to keep a constant set-point more than re-optimization. Thus, to design a control system, we specify the optimal operation and assume that the optimal operation of the system can be quantified in terms of a cost function J, which is to be minimized with respect to the degrees of freedom u, computed by the steady state behavior of the system

$$\min_{u} J(x,u,d) \tag{3.24}$$

$$\text{Subject to} \quad g_1(x,u,d) = 0$$

$$g_2(x,u,d) \leq 0$$

where x represents the state variables, u represents the independent variable that we can affect (degree of freedom), d represents all of the disturbances that we cannot impact, contains changes that impact to the system, changes in the process model, and changes in the inputs constraints.

To accomplish the controlled variable, the steady state economic loss (L) is evaluated as the difference between the actual value of a given cost function and the truly optimal value of the cost function, that is

$$L(u,d) = J(u,d) - J_{opt}(d) \tag{3.25}$$

A loss (L) value has to be small because it implies that the system is operating close to its optimum. Moreover, the flat optimum of the objective function has to be selected in order that an implementation error will obtain a small value of loss. Among optimization, active constraint control active that must be selected as controlled outputs because it is optimal to keep them constant at their set-points. The unconstrained degrees of freedom must be altered from the variables which obtain the smallest loss with the active constraints implemented. A selecting controlled variable that keeps the operation constant by using self-optimizing control has to satisfy the following requirements:

- The good controlled variable does not respond to the disturbances.
- The good controlled variable responds to changes in the manipulated variable.
- If there are more controlled variables, the good controlled variable does not relate with the other controlled variables.

- The good controlled variable is tractable.

The main steps of this procedure are as follows (Skogestad 2004):

- Degree of Freedom Analysis are defined. The way is to count the number of manipulated variables and discount the number of variables with no steady state that need to be controlled.

- The optimal operation problem is specified by formulating a scalar cost function *J* to be minimized with respect to the constraints.

- Important Disturbances are defined. Disturbances contain the impact of changes in the model, disturbances of process, and implementation errors in the controlled variables.

- Candidate controlled variables are specified by selecting active constraints which is controlled for all disturbances and choosing the other variables are the unconstrained candidates which obtain the smallest loss (L).

- The steady-state optimization problem is solved both the nominal case and the all disturbances to find the optimal cost.

- Therefore, the loss (L) is evaluated by altering sets of controlled variables. The loss is the difference between the actual value of a given cost function and the truly optimal value of the cost function.

Many candidate controlled variables give an acceptable loss. A selecting controlled variable which keep the operation constant at set-point (self-optimizing control) have to satisfy the following requirements. The variable is not be easy to change in the disturbances. The variable should be tractable and easy to changes in the manipulated variable. If there is more than one variable, the selecting controlled variable should not **relate with the others**.

3.4 Model Predictive Control (MPC)

Model Predictive Control (MPC) is an advanced method of process control that has been in use in the process industries in chemical plants. MPC also known as receding horizon control or moving horizon control uses a dynamic model of process

to predict the effect of the manipulated variables on the output and controlled variables obtained by minimizing the cost function. This predication considers both the inputs and outputs constraints of the process. An optimal input sequence is calculated. Then the predicted outputs are sent back to the controller, and a new optimizing problem is solved. The difference between the measured output and the predicted output is also sent to the controller to reduce offset. Block diagram for the MPC implementation is shown in Figure 3.5.

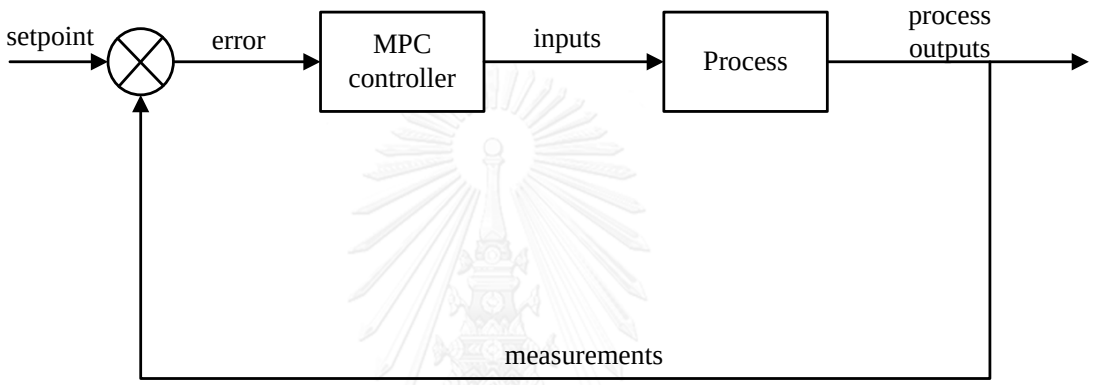

Figure 3.5 Block diagram for the MPC implementation

3.4.1 MPC Algorithm

MPC is based on iterative and shown in Figure 3.6. At certain sampling time k, MPC compute a set of control inputs [$u(k/k)$, $u(k+1/k)$ … $u(k+m-1/k)$],which consists of the current input $u(k)$ and m-1 future inputs. The inputs are computed until the set of the predicted outputs [$y(k+1/k)$ $y(k+2/k)$ … $y(k+p/k)$] reach the trajectory. The optimization is solved taking into consideration constraints on the outputs and inputs. Only the first control input $u(k/k)$ is implemented on the process over the interval [k,k]. At the next sampling time $y(k+1)$ is measured and step 1 to 3 is repeated and then $u(k+1/k+1)$ is computed.

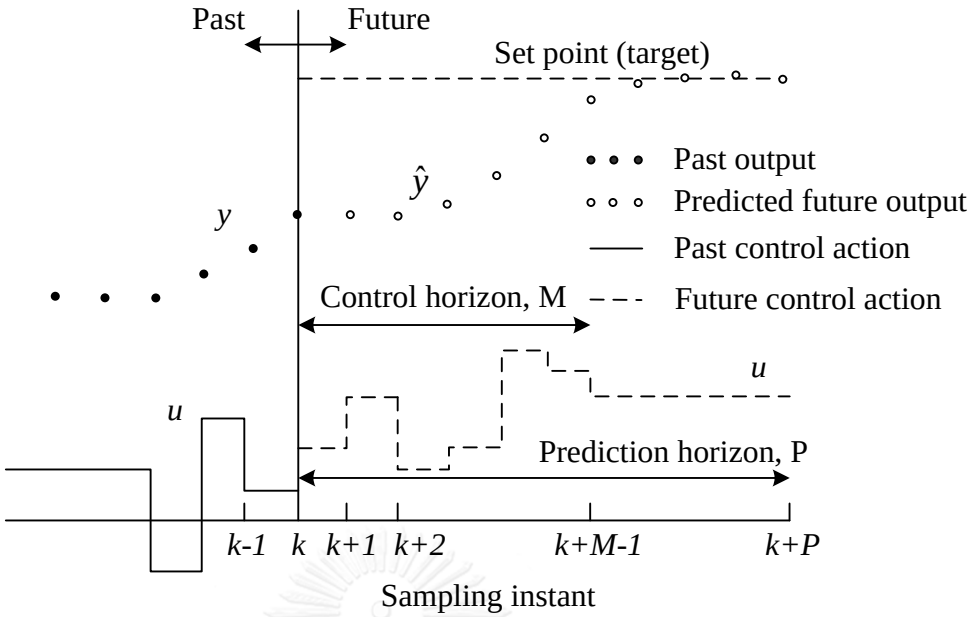

Figure 3.6 Concepts for model predictive control (Seborg, Mellichamp et al. 2010)

3.4.2 MPC Formulation

The model of the plant is described by the linear discretized time invariant model

$$\begin{aligned} x(k+1) &= Ax(k) + Bu(k) \\ y(k) &= C(k) \end{aligned} \tag{3.26}$$

where $x(k)$ denotes the state of the plant, $y(k)$ denotes the plant output, $u(k)$ denotes the control input. The control inputs $u(k+i/k), i=0,1,...,m-1$ are computed by minimizing a nominal cost $J_p(k)$ over a prediction horizon p as follows:

$$\min_{u(k+i/k),i=0,1...,m-1} J_p(k) \tag{3.27}$$

$$J_p(k) = \sum_{i=0}^{p} [x(k+i/k)^T \Theta x(k+i/k) + u(k+i/k)^T Ru(k+i/k)] \tag{3.28}$$

where $\Theta > 0$ and $R > 0$ are state and control weighting matrices respectively. Subject to constraints on the control inputs $u(k+i/k), i=0,1,...,m-1$ and on the state $x(k+i/k), i=0,1,..., p$ and the output $y(k+i/k), i=0,1,..., p$.

3.4.3 Problem Statement

One of the main advantages of MPC is able to handle constraints of the system during the design of the control loop. On the other hand, there are differences between the nominal model and the actual behavior of the process that caused the lack of guaranteed stability and robustness, then the performance of the control loop perform poorly and the optimization problem may become unfeasible. Another drawback of the MPC algorithms is the computation time which limited the use of MPC to plants with a slow response because it solves optimization problem in each sample time. Hence, Robust Model Predictive Control is proposed by Kothare et al., 1996 is attention. Since it can be guaranteed the robust stability of the closed loop system by minimizing an upper bound on the worst-case objective function subject to input and output constraints over Linear Matrix Inequality (LMI). The detail information will be introduced in the next section.

3.5 Robust Model Predictive Control (robust MPC)

In this section, a robust MPC of polytopic uncertain systems is presented. This describes the min-max approach that finds an upper bound or worst-case value of the cost function by maximizing it under the bound uncertainties and then computes the optimal solution by minimizing the upper bound. (Kothare, Balakrishnan et al. 1996)

3.5.1 Model for Uncertain Systems

Model for the uncertain systems considered is the linear time-varying system with polytopic uncertain as follows:

$$\begin{aligned} x(k+1) &= A(k)x(k) + B(k)u(k) \\ y(k) &= Cx(k) \\ A(k)\ B(k)\ &\in \Omega \end{aligned} \tag{3.29}$$

The uncertainties of the system are defined on system matrics $A(k)$ and $B(k)$ with the polytope set Ω that is

$$\Omega = Co \quad A_1 \quad B_1 \;,\; A_2 \quad B_2 \;,\cdots,\; A_L \quad B_L \tag{3.30}$$

where Co denotes the convex hull, $A_i \quad B_i$ are vertices of the convex hull. Mathematically, Ω can be written as $A(k) \quad B(k) = \sum_i^L \lambda_i \; A_i \quad B_i$ such that $\sum_i^L \lambda_i(k) = 1$ and $\lambda_i(k) \geq 0$.

The objective is to design the state feedback control law, $u(k+i) = Kx(k+i|k), \quad i > 0$, $K = YQ^{-1}$ is able to guarantee both robust stability and constraint satisfaction within a positive invariant set, and can be calculated by solving the following optimization problem

$$\min_{u(k+i|k),i=0,1,...,m} \quad \max_{A(k+i)\;\; B(k+i)\;\in\Omega, i\geq 0} \quad J_\infty(k) \tag{3.31}$$

$$J_\infty(k) = \sum_{i=0}^{\infty} [x(k+i|k)^T \Theta x(k+i|k) + u(k+i|k)^T R u(k+i|k)] \tag{3.32}$$

The optimization problem is subject to the model uncertainty, $x(k+1) = A(k)x(k) + B(k)u(k)$ and

$$\left|u_h(k+i/k)\right| \leq u_{h,\max}, h = 1,2,3,...,n_u \tag{3.33}$$

$$\left|y_m(k+i/k)\right| \leq y_{m,\max}, m = 1,2,3,...,n_y \tag{3.34}$$

Derivation of Upper Bound

The quadratic cost function is defined as below

$$J_{\infty}(k) = \sum_{i=0}^{\infty} [x(k+i|k)^T \Theta x(k+i|k) + u(k+i|k)^T Ru(k+i|k)] \tag{3.35}$$

By using min-max approach the optimization problem is formulated as follow

$$\min_{u(k+i|k),i=0,1,...,m} \quad \max_{A(k+i)\ B(k+i)\ \in \Omega, i \geq 0} J_{\infty}(k) \tag{3.36}$$

To find an upper bound on $J_{\infty}(k)$, then we can design the controller such that the upper bound is minimized respect to the model uncertainty. Then, it is assumed that we defined a quadratic function $V(x(k/k)) = x(k/k)^T Px(k/k)$ at sampling time k, where P is a parameter dependent positive definite matrix. For any $A(k)\ B(k)\ \in \Omega, i \geq 0$, suppose that $V(x(k/k))$ satisfies the following robust stability constraint:

$$\begin{aligned} &V(x(k+i+1/k)) - V(x(k+i/k)) \\ &\quad \leq -[x(k+i/k)^T \Theta x(k/k) + u(k+i/k)^T Ru(k/k)] \end{aligned} \tag{3.37}$$

As it is assumed that the summation is up to ∞, i.e., i → ∞, $x(i/k)$ should approach zero, that is $x(\infty/k) = 0$. Summing from i = 0 to ∞ leads to the following inequality

$$\max_{A(k+i)\ B(k+i)\ \in \Omega, i \geq 0} J_{\infty}(k) \leq V(x(k/k)) \tag{3.38}$$

From the above inequality, it shows that $V(x(k/k))$ is an upper bound on $J_{\infty}(k)$ and the optimization problem can be reformulated as

$$\min_{u(k+i),i=1,2,...,\infty} V(x(k)) \tag{3.39}$$

which still depends on the uncertainties. This leads to the optimization involving Linear Matrix Inequality (LMI). LMI is a convex constraint. Consequently, the optimization problems with convex objective functions and LMI constraints are efficiently solvable and it is tractable. In addition, the LMI is suitable to handle uncertain systems and input/output constraints. The LMI and the LMI-based optimization are described in the following section.

3.5.2 Linear Matrix Inequality (LMI)

The main concept of the LMI approach is that at each time instant, an LMI optimization problem is solved that relate to input and output constraints and the explanation of the plant uncertainty and guarantees robust stability.

Definition 1: A linear matrix inequality is a matrix inequality of the form

$M(x) = M_0 + \sum_{i=1}^{l} x_i M_i > 0$, where $x_i \in R^l$ is the variable, and $M_i = M_i^T \in \mathbb{R}^{n \times n}$.

$M(x) > 0$ means as a single LMI: $diag(M_1(x),...,M_n(x)) > 0$

Definition 2: The LMI-based optimization is formulated as:

$$\begin{aligned} &\min c^T x \\ &s.t.\ M(x) > 0 \end{aligned} \tag{3.40}$$

where M is a symmetric matrix the depends on the optimization variable x, and c is a real vector of appropriate size.

Lemma 1 (Schur complements)

$$\begin{bmatrix} Q & S \\ S^T & R \end{bmatrix} > 0 \text{ where } Q = Q^T, R = R^T \tag{3.41}$$

$$R > 0,\ Q - SR^{-1}S^T > 0 \tag{3.42}$$

$$Q > 0,\ R - S^T Q^{-1} S > 0 \tag{3.43}$$

Also, if $Q = Q^T > 0$, then

$$\begin{bmatrix} Q & S \\ S^T & R \end{bmatrix} \geq 0 \text{ where } R = R^T \quad \Leftrightarrow \quad R \geq 0,\ R - S^T Q^{-1} S \geq 0 \tag{3.44}$$

and if $R = R^T > 0$, then

$$\begin{bmatrix} Q & S \\ S^T & R \end{bmatrix} \geq 0 \text{ where } Q = Q^T \quad \Leftrightarrow \quad Q \geq 0,\ Q - S R^{-1} S^T \geq 0 \tag{3.45}$$

The lemma 1 can transform nonlinear matrix inequalities to linear matrix in inequalities (LMIs). For more detail in Appendix A.

3.5.3 Robust Model Predictive Control

In this section, an LMI approach is presented based on parameter dependent Lyapunov functions for the robust MPC problem defined as follows

Theorem 1: Consider the polytopic uncertain system, and $x(k/k)$ refers to the state measured at sampling time k. Then, the state feedback matrix K the controller that minimizes the upper bound $V(x(k/k))$ is given by

$$K = YQ^{-1} \tag{3.46}$$

where Y and Q are obtained from the following convex optimization problem:

$$\min_{\gamma,Y,Q} \ \gamma$$

$$\text{subject to} \quad \begin{bmatrix} 1 & x(k|k)^T \\ x(k|k) & Q \end{bmatrix} \geq 0$$

$$\begin{bmatrix} Q & QA_j^T + Y^T B_j^T & Q\Theta^{\frac{1}{2}} & Y^T R^{\frac{1}{2}} \\ A_j Q + B_j Y & Q & 0 & 0 \\ \Theta^{\frac{1}{2}} Q & 0 & \gamma I & 0 \\ R^{\frac{1}{2}} Y & 0 & 0 & \gamma I \end{bmatrix} \geq 0, \ j = 1, 2, ..., L \tag{3.47}$$

Proof Minimization of $V(x(k/k)) = x(k/k)^T P x(k/k)$, P > 0, is equivalent to

$$\begin{aligned} &\min_{\gamma,p} \quad \gamma \\ &s.t \quad x(k|k)^T P x(k|k) \leq \gamma \end{aligned} \tag{3.48}$$

Defining Q = γP $^{-1}$ > 0 and using the Schur complements, we obtain that this is equivalent to

$$\begin{aligned} &\min_{\gamma,p} \quad \gamma \\ &s.t \quad \begin{bmatrix} 1 & x(k|k)^T \\ x(k|k) & Q \end{bmatrix} \geq 0 \end{aligned} \tag{3.49}$$

From The quadratic function V is required to satisfy. By substituting $u(k+i) = Kx(k+i|k), \quad i > 0$ and the polytopic uncertain system $x(k+1) = A(k)x(k) + B(k)u(k)$ then substituting P=γQ^{-1}, pre-multiplying by Q^{T}, post multiplying by Q, substituting $K = YQ^{-1}$, and applying Schur complement to the resulting inequality, we obtain

$$\begin{bmatrix} Q & QA_j^T + Y^T B_j^T & Q\Theta^{\frac{1}{2}} & Y^T R^{\frac{1}{2}} \\ A_j Q + B_j Y & Q & 0 & 0 \\ \Theta^{\frac{1}{2}} Q & 0 & \gamma I & 0 \\ R^{\frac{1}{2}} Y & 0 & 0 & \gamma I \end{bmatrix} \geq 0,\ j = 1,2,...,L \qquad (3.50)$$

The feedback matrix is then given by $K=YQ^{-1}$

Input and Output Constraints

In this section, input and output constraints are presented into the optimization problem and show that the solution of the optimization respect with input and output constraints guarantee robust stability.

Input Constraints

Obtained $\|u(k+i|k)\|_2 \leq u_{\max}, i \geq 0$ and using Schur complements, the LMI:

$$\begin{bmatrix} u_{\max}^2 I & Y \\ Y^T & Q \end{bmatrix} \geq 0 \qquad (3.51)$$

Output Constraints

Consider

$$\max_{[A(k+j)B(k+j)\in\Omega, j\geq 0]} \|y(k+i|k)\|_2 \leq y_{,\max}, i \geq 1 \qquad (3.52)$$

The following LMI:

$$\begin{bmatrix} Q & (A_j Q + B_j Y)^T C^T \\ C(A_j Q + B_j Y) & y_{\max}^2 I \end{bmatrix} \geq 0,\ j = 1,2,3...,L \qquad (3.53)$$

Finally, the optimization problem can be expressed as the LMI- based optimization problem. The cost function is presented as follows:

$$\min_{\gamma,Y,Q} \ \gamma$$

$$\textit{subject to} \quad \begin{bmatrix} 1 & x(k|k)^T \\ x(k|k) & Q \end{bmatrix} \geq 0 \tag{3.54}$$

$$\begin{bmatrix} Q & QA_j^T + Y^T B_j^T & Q\Theta^{\frac{1}{2}} & Y^T R^{\frac{1}{2}} \\ A_j Q + B_j Y & Q & 0 & 0 \\ \Theta^{\frac{1}{2}} Q & 0 & \gamma I & 0 \\ R^{\frac{1}{2}} Y & 0 & 0 & \gamma I \end{bmatrix} \geq 0, \ j = 1,2,...,L \tag{3.55}$$

$$\begin{bmatrix} u_{\max}^2 I & Y \\ Y^T & Q \end{bmatrix} \geq 0 \tag{3.56}$$

$$\begin{bmatrix} Q & (A_j Q + B_j Y)^T C^T \\ C(A_j Q + B_j Y) & y_{\max}^2 I \end{bmatrix} \geq 0, \ j = 1,2,3...,L \tag{3.57}$$

Eq. 3.54 is a construction of an invariant ellipsoid for guaranteeing the trajectory of outputs, eq. 3.55 is expressed for guaranteeing robust stability, eq. 3.56 is expressed for guaranteeing input constraint satisfaction and eq. 3.57 is expressed for guaranteeing output constraint satisfaction.

CHAPTER IV

DYNAMIC MODELING OF A POLYMER EXCHANGE MEMBRANE FUEL CELL

The PEMFC system model is analytically described in this section. The dynamic models of the PEMFC are highly nonlinear and it depends on the operation conditions, such as temperature, pressure, current density, etc. A dynamic model can help better understanding the dynamic behavior of PEMFC system, and it is important for the control design.

4.1 PEMFC System Description

The work is performed on a nonlinear dynamic model of a PEMFC proposed by Amphlett et al. (1996) and Khan MJ (2005). It is a lumped model that describes quite well the system dynamics. Hydrogen is fed in the anode side of the fuel cell and its excess gas can be removed, while the air used as the oxidant is kept flowing through the stack, and the temperature of water flow rate at the inlet is changed by the external heat exchanger device as shown Figure 4.1.

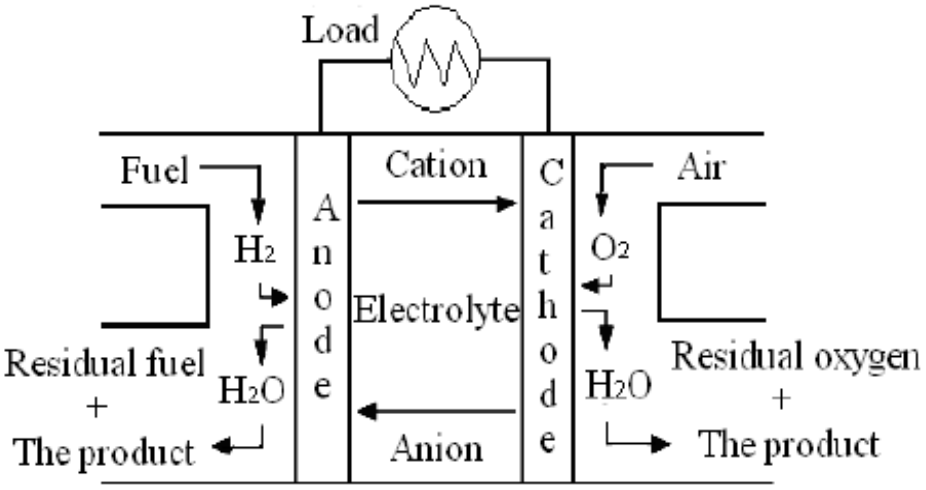

Figure 4.1 Flow sheet of the PEMFC system

4.2 PEMFC Mathematical Model

The dynamic mathematical models for the PEMFC in this work include the mass balances for describing gas variation, the energy balance and the electrochemical model. Detailed model equations are described in following sections. Several assumptions are made as below:

1. Fuel cell performs lumped model.

2. All gases are the ideal gas law. It is assumed that pure hydrogen (99.99%) is fed to the anode, and air that is uniformly mixed with nitrogen and oxygen by a ratio of 21:79 is supplied to the cathode.

3. The temperature of hydrogen at the anode and oxygen at the cathode are equal to the cell temperature.

4. The reactant gases are saturated with vapor and the membrane is fully saturated with water.

4.2.1 Reactant Flow Model

The transient dynamic in anode and cathode channels are studied in this study. In the anode channel modeling, it is simplified by assuming pure hydrogen flows into the channel. In addition, partial hydrogen diffuses through anode electrode into the anode active layer where it is consumed by the electrochemical reaction. Therefore, the dynamic of the partial pressure of hydrogen at anode is obtained as follow:

$$\frac{dp_{H_2}}{dt} = \frac{RT}{V_{an}}\left(\dot{m}_{H_2,in} - k_{an}(p_{H_2} - p_{atm}) - \frac{jA_{act}}{2F} \right) \tag{4.1}$$

The dynamic of the partial pressure of oxygen at cathode is similar to the anode control volume, which oxygen in air flow into the channel.

$$\frac{dp_{O_2}}{dt} = \frac{RT}{V_{ca}}\left(\dot{m}_{O_2,in} - k_{ca}(p_{O_2} - p_{atm}) - \frac{jA_{act}}{4F} \right) \tag{4.2}$$

where $\dot{m}_{H_2,in}$ is the inlet flow rate of hydrogen, $\dot{m}_{O_2,in}$ is the inlet flow rate of oxygen ,T is the cell temperature (K), j is the operating cell current density (A/cm^2), p_{H_2} and p_{O_2} are the partial pressures of hydrogen and oxygen (atm), respectively. p_{atm} is the ambient pressure (atm). R is the gas constant (J/mol/K), F is Faraday constant (C/mol), A_{act} is the active area (cm^2), k_{an} and k_{ca} are mass flow rate coefficients (mol/s.atm).

4.2.2 Thermal Model of a PEMFC

The heat produced from the electrochemical reaction is one of the important problems for PEMFC. When PEMFC is operated, the temperature increases highly which causes membrane degradation. In this study, the temperature is defined as one of the state variables and a control strategy is developed for studying the transient thermal behavior of a PEMFC. Therefore two main assumptions are introduced in the energy balances. Firstly, any fuel energy that is not converted into electrical energy is converted into heat and secondly, the temperature at the anode and cathode side is equal to the fuel cell stack temperature. The energy model of a PEMFC is using the main terms of the overall energy balance using the following principle

$$\begin{bmatrix}\text{Change in}\\ \text{the total energy}\\ \text{of the system}\end{bmatrix} = \begin{bmatrix}\text{Total energy}\\ \text{entering}\\ \text{the system}\end{bmatrix} - \begin{bmatrix}\text{Total energy}\\ \text{leaving}\\ \text{the system}\end{bmatrix}$$

$$C_t \frac{dT}{dt} = P_{tot} - \dot{Q}_{elec} + \dot{Q}_{in} - \dot{Q}_{out} - \dot{Q}_{cool} - \dot{Q}_{loss} \tag{4.3}$$

The total energy from the electrochemical reaction in a PEMFC is calculated by the product of the energy of reaction (ΔH) and the reacted hydrogen molar flow rate $\left(\dot{m}_{H_2,react}\right)$. The associated equation is:

$$P_{tot} = \frac{I}{2F}\Delta H \tag{4.4}$$

where I represents the cell current (A). The electrical power output generated by the fuel cell is expressed as,

$$\dot{Q}_{elec} = VI \tag{4.5}$$

Heat loss at the stack surface is described as,

$$\dot{Q}_{loss} = \frac{T - T_{amb}}{R_t} \tag{4.6}$$

The input heat flow rate by the reactants is described as,

$$\begin{aligned}\dot{Q}_{in} = &(\dot{m}_{H_2,in} c_{p,H_2} + \dot{m}_{H_2O,an,in} c^{g}_{p,H_2O})(T_{an,in} - T_o) \\ &+ (\dot{m}_{O_2,in} c_{p,O_2} + \dot{m}_{N_2,in} c_{p,N_2} + \dot{m}_{H_2O,ca,in} c^{g}_{p,H_2O})(T_{ca,in} - T_o)\end{aligned} \tag{4.7}$$

where c_{p,O_2} denotes the specific heat of oxygen (J/mol/K) , c_{p,H_2} denotes the specific heat of hydrogen (J/mol/K), c_{p,N_2} denotes the specific heat of nitrogen (J/mol/K), c^{g}_{p,H_2O} denotes the specific heat of gaseous water (J/mol/K), and c^{liq}_{p,H_2O} denotes the specific heat of liquid water (J/mol/K). $T_{\text{air},in}$ denotes temperature of air (K), and $T_{\text{H}_2,in}$ denotes temperature of hydrogen (K). The input vapor molar flow rate at anode side is described as,

$$\dot{m}_{H_2O,an,in} = \left[\frac{\varphi_{an} p_{sat}(T_{an,in})}{p_{an} - \varphi_{an} p_{sat}(T_{an,in})}\right] \dot{m}_{H_2,in} \tag{4.8}$$

The input vapor molar flow rate at cathode side is described as,

$$\dot{m}_{H_2O,ca,in} = \left[\frac{\varphi_{ca} p_{sat}(T_{ca,in})}{p_{ca} - \varphi_{ca} p_{sat}(T_{ca,in})}\right] \dot{m}_{air,in} \tag{4.9}$$

The outlet heat flow rate by the reactants is described as,

$$\begin{aligned}\dot{Q}_{out} = &(\dot{m}_{H_2,out} c_{p,H_2} + \dot{m}_{H_2O,an,out} c^{g}_{p,H_2O} \\ &+ \dot{m}_{O_2,out} c_{p,O_2} + \dot{m}_{N_2,out} c_{p,N_2} + \dot{m}_{H_2O,ca,out} c^{g}_{p,H_2O} + \dot{m}^{gen}_{H_2O,ca,out} c^{liq}_{p,H_2O})(T - T_o)\end{aligned} \tag{4.10}$$

The water generation rate is described as,

$$\dot{m}^{gen}_{H_2O,ca,out} = \frac{jA_{act}}{2F} \tag{4.11}$$

The output vapor molar flow rate at anode side is described as,

$$\dot{m}_{H_2O,an,out} = \dot{m}_{H_2O,an,in} - \left[\frac{\varphi_{an} p_{sat}(T)}{p_{an} - \varphi_{an} p_{sat}(T)}\right] \dot{m}_{H_2,react} \tag{4.12}$$

The output vapor molar flow rate at cathode side is described as,

$$\dot{m}_{H_2O,ca,out} = \dot{m}_{H_2O,ca,in} - \left[\frac{\varphi_{ca} p_{sat}(T)}{p_{ca} - \varphi_{ca} p_{sat}(T)}\right] \dot{m}_{O_2,react} \tag{4.13}$$

4.2.3 Electrochemical Model

Fuel cell voltage means the performance of a PEMFC. Under its operation the PEMFC typically produces 0.5-0.8 V based on the polarization V-I curve which is the relationship between the voltage and the load current. To obtain the higher voltage, multiple cells are connected in series. Then, the output voltage of a single PEMFC including activation, ohmic and concentration losses can be defined as the following expression.

$$V_{cell} = E - V_{act} - V_{ohm} - V_{con} \tag{4.14}$$

where V_{cell} represent the output voltage of the PEMFC, E represents the thermodynamic potential or the reversible voltage of the cell, V_{act} denotes the voltage drop due to the activation losses of the anode and cathode, V_{ohm} denotes the ohmic voltage form the resistance of proton though membrane and V_{con} denotes voltage drop resulting from the decrease of concentration of the reactants gases.

The reversible voltage is the thermodynamic potential of the fuel cell obtained in an open circuit thermodynamic balance. For the PEMFC, it is calculated from the Nernst equation as follow:

$$E = 1.229 - 8.5\times10^{-4}(T - 298.15) + \frac{RT}{2F}\ln\left[p_{H_2} p_{O_2}^{0.5}\right] \tag{4.15}$$

It is noted that the membrane temperature and the partial pressures of gases depend on the cell current: increasing current, the partial pressures of gases decrease whereas temperature increases.

The activation losses caused by the slowness of the reactions taking place on the surface of the electrodes, can be calculated by

$$V_{act} = -[\xi_1 + \xi_2 T + \xi_3 T \ln\left(c_{O_2}\right) + \xi_4 T \ln\left(I\right)] \tag{4.16}$$

This description for the activation overvoltage takes into account the concentration of oxygen at the catalyst layer and various experimentally defined parametric coefficients, ξ,

$$\begin{aligned} \xi_1 &= -0.948 \\ \xi_2 &= 0.00286 + 0.0002\ln(A) + 4.3\times10^{-5}\ln(c_{H_2}) \\ \xi_3 &= 7.6\times10^{-5} \\ \xi_4 &= -1.93\times10^{-4} \end{aligned} \tag{4.17}$$

where c_{O_2} is the concentration of oxygen in the catalytic interface of cathode and c_{H_2} is the concentration of hydrogen in the catalytic interface of anode as form

$$c_{O_2} = 1.97\times10^{-7}\times p_{O_2}\times\exp(\frac{498}{T}) \tag{4.18}$$

$$c_{H_2} = 9.174\times10^{-7}\times p_{H_2}\times\exp(\frac{-77}{T}) \tag{4.19}$$

The term ξ are semi-empirical coefficients, defined by the following equation:

$$\xi_1 = \left(\frac{-\Delta G_a}{a_c nF}\right) + \left(\frac{-\Delta G_c}{2F}\right) \tag{4.20}$$

$$\xi_2 = \frac{R}{a_c nF}\left[\ln nFAk_c^0 (C_{H^+})^{(1-\alpha_c)}(C_{H_2O})\right] + \frac{R}{2F}\left[\ln 4FAk_a^0 (C_{H_2})\right] \tag{4.21}$$

$$\xi_3 = \frac{R}{a_c nF}(1-a_c) \tag{4.22}$$

$$\xi_4 = -\left(\frac{R}{a_c nF} + \frac{R}{2F}\right) \tag{4.23}$$

where ΔG_a represents free activation energy for the standard state (J/mol) referred to the anode, ΔG_c represents free activation energy for the standard state (J/mol) referred to the cathode, a_c represents parameter for the cathode chemical activity, k_a^o, k_c^o represent intrinsic rate constant for the anode and cathode reactions, respectively (cm/s), C_{H^+} represents proton concentration at the cathode membrane/gas interface (mol/cm^3), C_{H_2} represents liquid phase concentration of hydrogen at anode/gas interface (mol/cm^3), and C_{H_2O} represents water concentration at the cathode membrane/gas interface (mol/cm^3).

The ohmic losses arise from resistance of membrane to the transfer of proton and the resistance of the electrode and collector plate to the transfer of electron. The ohmic losses is determined by

$$V_{ohmic} = IR_{\text{int}} \tag{4.24}$$

$$R_{\text{int}} = \frac{181.6\ell_{mem}\left[1 + 0.03\left(\frac{I}{A_{act}}\right) + 0.062\left(\frac{T}{303}\right)^2\left(\frac{I}{A_{act}}\right)^{2.5}\right]}{A_{act}\left[\psi - 0.634 - 3\left(\frac{I}{A_{act}}\right)\right]\exp\left[4.18\left(\frac{T-303}{T}\right)\right]} \tag{4.25}$$

where ℓ_{mem} is the membrane thickness. ψ is the water content in membrane. This parameter depends on the membrane fabrication process and the stoichiometric rate of the gas in the anode.

The concentration losses are the result of mass transport of gases to the reaction. The mass transport affects the concentrations of hydrogen and oxygen. This causes a decrease of the partial pressure of gases. Therefore the voltage due to the mass transport is expressed as:

$$V_{con} = -\frac{RT}{2F}\ln\left(1-\frac{j}{j_{\max}}\right) \tag{4.26}$$

where j_{max} is defined as a maximum current density which is in range from 1000 to 1500 mA/cm^2.

4.3 Solution Method

In this study, the dynamic models of the PEMFC are solved by the MATLAB simulation tool and the set of equations is solved by ODE method. Model parameters of PEMFC are shown in Table 4.1 and operating condition of PEMFC are shown in Table 4.2. The solution strategy is as follow:

1. Determine operating conditions, and initial conditions
2. Calculate voltage by initial input values
3. Solve total mass balance and energy balance equations
4. Calculate the new cell temperature, and partial pressure of hydrogen and oxygen from all ordinary differential equation.
5. For the next step, go to step 2, those value got from step 4 as the initial values and repeat the process until reach the end of time period.

Table 4.1 Model parameters of PEMFC

Parameters	Symbol	Value
Cell active area, cm^2	A_{act}	232
Anode volume, m^3	V_{an}	0.005
Cathode volume, m^3	V_{ca}	0.01
Flow constant at anode, $mols^{-1}$ atm	k_{an}	0.065
Flow constant at cathode, $mols^{-1}$ atm	k_{ca}	0.065
Membrane thickness, cm	ℓ_{mem}	178×10^{-4}
Hydrogen enthalpy of combustion, $kJmol^{-1}$	ΔH	285.5
Thermal capacitance, kJ K^{-1}	C_t	17.9
Thermal resistance, K W^{-1}	R_t	0.115
Membrane water content	ψ	14

Table 4.2 Operating parameters for PEMFC

Parameters	Symbol	Value
Temperature of hydrogen, K	$T_{H2,in}$	348
Temperature of air, K	$T_{air,in}$	348
Relative humidity of reactants, %	φ	100

4.4 Simulation Results

4.4.1 Model Validation of a PEMFC

To confirm the PEMFC model including the mass balances for describing gas variation, the energy balance and the electrochemical model as proposed in previous section can reliably predict the performance of the PEMFC. The simulated polarization curve is compared with the experimental data reported in the literature of Mueller, Brouwer et al. (2007). In their experiment, an operating temperature of PEMFC is at 343 K and the operating pressure is 1 atm. Relative humidity and temperatures of both hydrogen and air are at 96% and 343 K. Hydrogen and air utilizations are 0.53 and 0.33, respectively. Comparison between the experimental and the simulated polarization curves under the range of current densities from 0 to 1 A/cm^2 are shown in Figure 4.2. It is observed that the simulated polarization curve shows a good agreement with the experimental polarization curve. However, there are variations of results between the simulated and experimental data curves in low current density region and highest current density region. The variation in the low current density region or the activation region is due to the estimation of some parameters affecting the activation regions, which are not useable in the model predictions. For the variation in the mass transport region, the simulated curve is shifted upward compared to the experimental data curve.

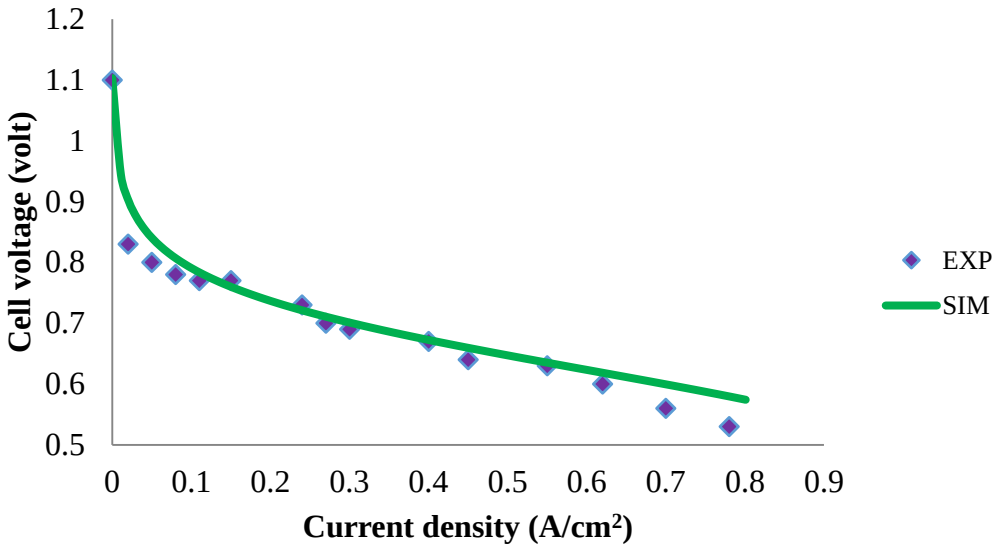

Figure 4.2 Comparison between the simulated polarization curves and the experimental polarization curve from Mueller, Brouwer et al. (2007)

4.4.2 Selection of Operating Conditions of a PEMFC

Selection of operating conditions for control design of PEMFC is very important to achieve the performance of fuel cells. In order to select operating conditions, the steady state analysis is performed for the PEMFC. The operating conditions are applied to be the initial condition for dynamic response and control design of PEMFC. Figure 4.3 – 4.4 show the cell voltage, power density and temperature as function of the current density. It is revealed that the current density increases with decreasing cell voltage and temperature. The cell temperature increases at high current density because the electrochemical reactions are more active. The cell voltage decreases immediately due to concentration losses. In this work, the operating points at steady state condition are selected. At current density of 0.51 A/cm^2, the voltage of 0.59 V for the power density of 0.30 W/cm^2 is found to be the optimal operation condition for the PEMFC and also the cell temperature equal to 332 K.

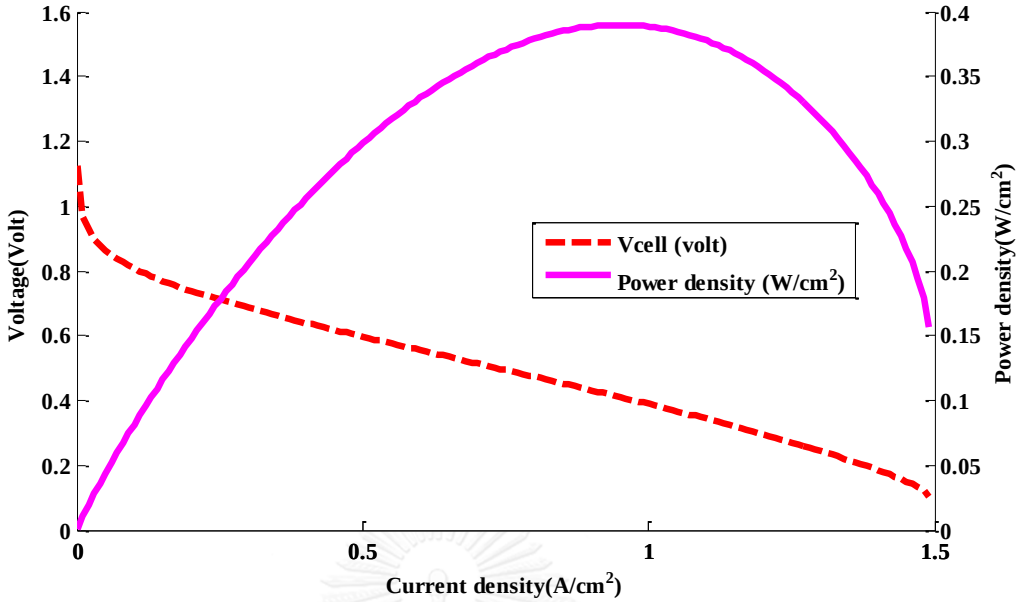

Figure 4.3 The cell voltage and power density as a function of the current density

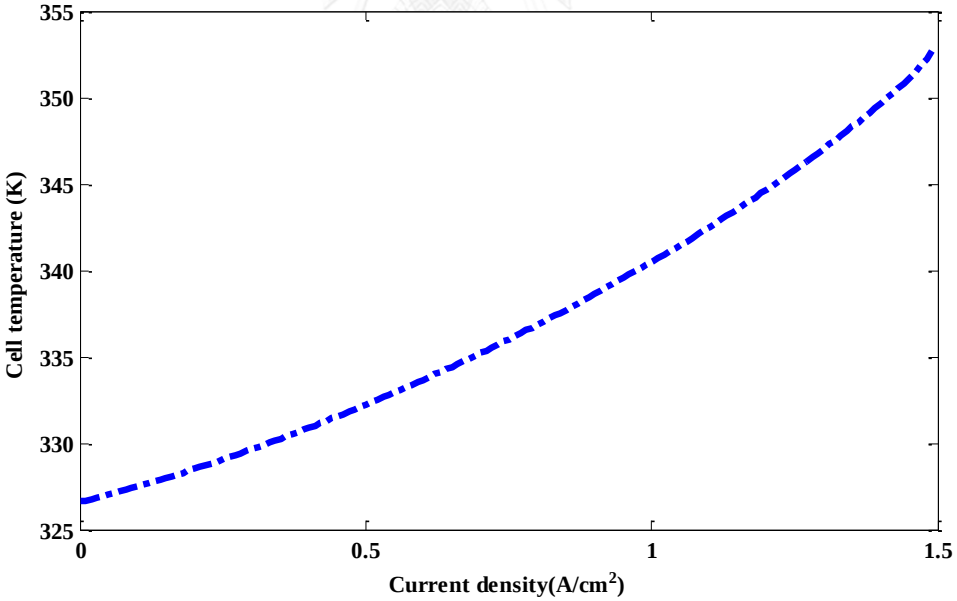

Figure 4.4 The cell temperature as a function of the current density

4.4.3 Dynamic Responses of a PEMFC under Various Operating Conditions

In this section, the dynamic responses of the cell voltage and cell temperature are discussed. Dynamic behavior is especially the most significant for fuel cell operation that should be studied under operating conditions such as temperature, flow

rate of the reactant gases etc. In addition, dynamic behavior is also critical to the control design of the PEMFC because control system is needed to provide that the flow rate and temperature of fuel and air are operated during normal operation at variable loads, as well as during system start-up and shut-down. Therefore, the operating points from previous section are applied to be the initial condition to investigate the responses of the cell voltage and cell temperature and to achieve stable performance under various inputs such as variation of current density, flow rates of hydrogen and air, and temperatures of hydrogen and air. The first period between 0 and 6,000 sec, the cell voltage and cell temperature is kept constant at their setpoints, 0.59 V and 332 K, respectively. Then, the step changes in the inputs are raised up at the second period. Finally, the step changes in the inputs are down at the last period.

4.4.3.1 Effect of a step change in current density

When a step changes in the current density is immediately increased from 0.51 A/cm^2 to 0.61 A/cm^2 at 6,000 sec, and then immediately decreased from 0.61 A/cm^2 to 0.41 A/cm^2 at 12,000 sec (Figure 4.5). Figure 4.6 display the transient responses of the cell voltage and cell temperature. When the current density is changed from 0.51 A/cm^2 to 0.61 A/cm^2, the voltage rapidly decreased from 0.59 V to 0.53 V and then, the voltage increased to its steady state value is 0.55 V. When the current density is changed from 0.61 A/cm^2 to 0.41 A/cm^2, the voltage suddenly increased from 0.55 V to 0.64 V, and then its steady state value is 0.63 V. To explain the voltage transient behavior, especially the undershoot phenomenon, since the rate of consumption reactant gas depends on the current density and fuel gas will be consumed more quickly when a higher current density is drawn out which lead to a greater concentration losses.

In addition, the transient response of the temperature is considered by changing the current density from 0.51 A/cm^2 to 0.61 A/cm^2 at 6,000 sec, as shown in Figure 4.6. The cell temperature increased from 333 K to 334 K and then the cell temperature reaches the steady-state value after a few seconds**.** Also, when the current density is changed from 0.61 A/cm^2 to 0.41 A/cm^2, the cell temperature decreased from 334 K to 331 K. Normally, the electrochemical reaction of fuel cell is more active at the high current density and the heat is released from the fuel cell. Therefore, the cell temperature variation depends on the step current density changes.

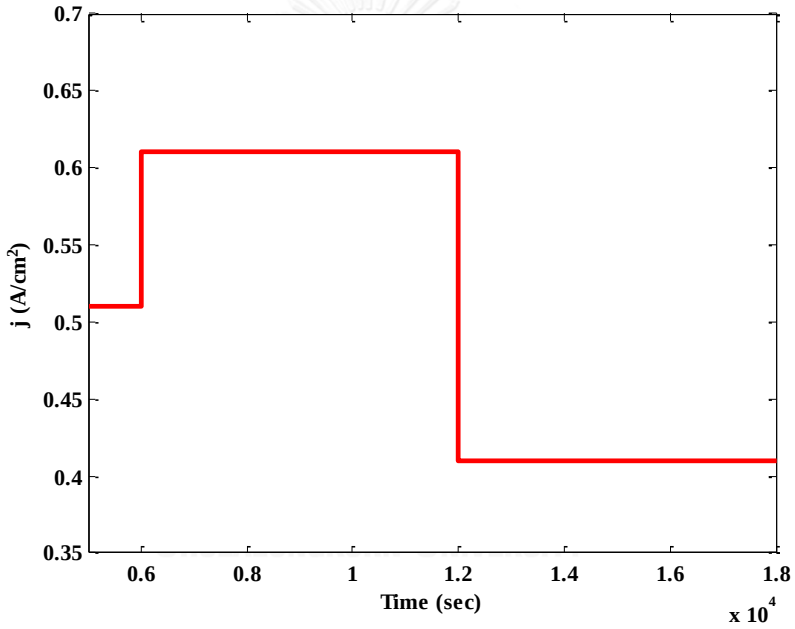

Figure 4.5 A step change in the current density

(a)

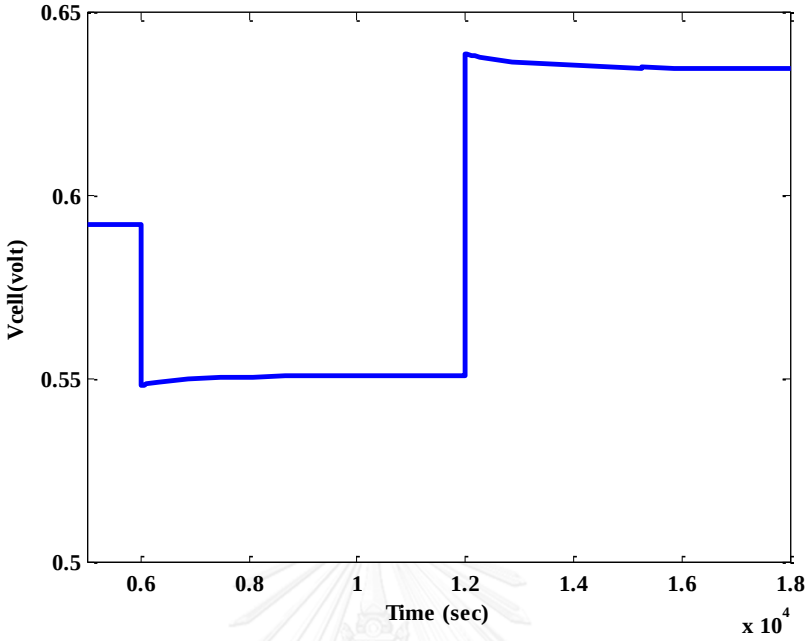

(b)

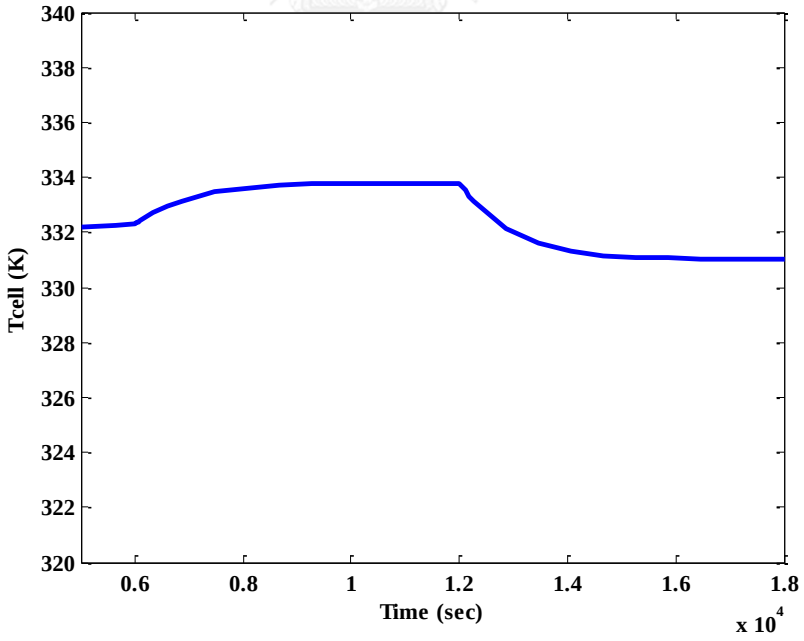

Figure 4.6 Transient responses as the current density; (a) cell voltage, (b) cell temperature

4.4.3.2 Effect of a step change in inlet flow rates of hydrogen and air

The transient responses of the cell voltage and cell temperature are investigated when the inlet flow rates of hydrogen and air change in Figure 4.7 - 4.10. Figure 4.7 display that when the inlet flow rate of hydrogen is changed from 0.023 mol/sec to 0.033 mol/sec, the voltage rapidly increased from 0.590 V to 0.598 V and the cell temperature increased from 332 K to 333 K. At 6,000 sec, the inlet flow rate of hydrogen is changed from 0.033 mol/sec to 0.013 mol/sec, the voltage suddenly decrease from 0.598 V to 0.588 V and the temperature is less variation. The results illustrate that the cell outputs respond to the changes of the molar hydrogen flow rate and reach a new steady state value. The fuel cell exhibits a good dynamic response of cell voltage at high hydrogen flow rate. The fuel cell shows that dynamic response of cell voltage is reduced at low hydrogen flow rate. Figure 4.8 implies that increasing the inlet flow rate of hydrogen can improve cell performance in term of cell voltage because high hydrogen flow rate can increase the partial pressure of hydrogen and membrane conductivity in fuel cell.

When the inlet flow rate of air is immediately increase from 0.27 mol/sec to 0.32 mol/sec at 6,000 sec, and then immediately decrease from 0.32 mol/sec to 0.22 mol/sec at 12,000 sec (Figure 4.9). Figure 4.10 displays the transient responses of cell voltage and cell temperature. When the inlet flow rate of air is changed from 0.27 mol/sec to 0.32 mol/sec, the cell voltage increase from 0.590 V to 0.598 V and the cell temperature also increase from 332 K to 333.9 K. When the inlet flow rate of air is changed from 0.32 mol/sec to 0.22 mol/sec, the voltage decrease from 0.598 V to 0.57 V and the cell temperature decrease from 333.9 K to 331 K. The results illustrate that the changes of the inlet flow rate of air influent on the cell outputs. The fuel cell exhibits good dynamic response at high inlet flow rate of air. The fuel cell exhibits that dynamic response is reduced at low inlet flow rate of air. Figure 4.10 implies that increasing the inlet flow rate of air can improve cell performance in term of cell voltage and cell temperature because high inlet flow rate of air improves partial pressure of oxygen and can remove the excess water. Also, it increases the oxygen mass transport in cathode side of fuel cell.

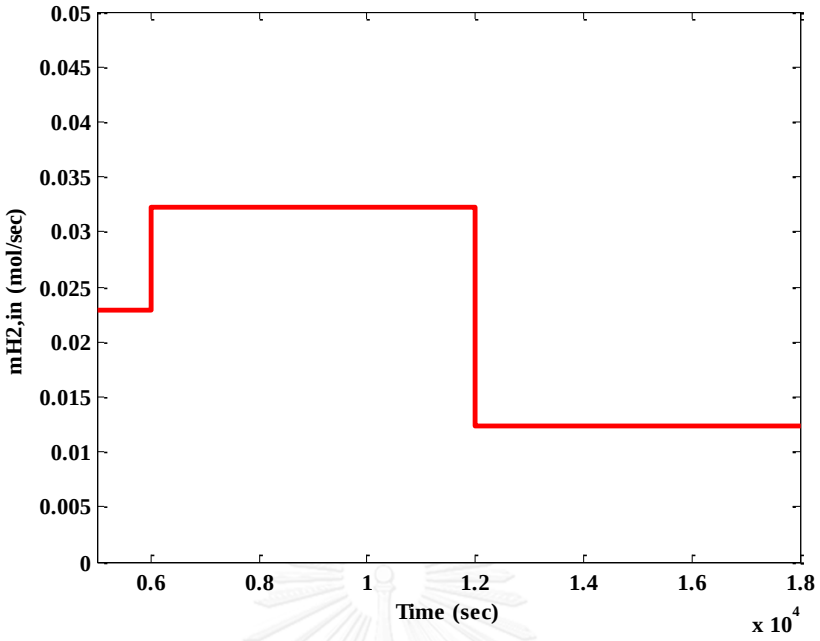

Figure 4.7 A step change in the inlet flow rate of hydrogen

(a)

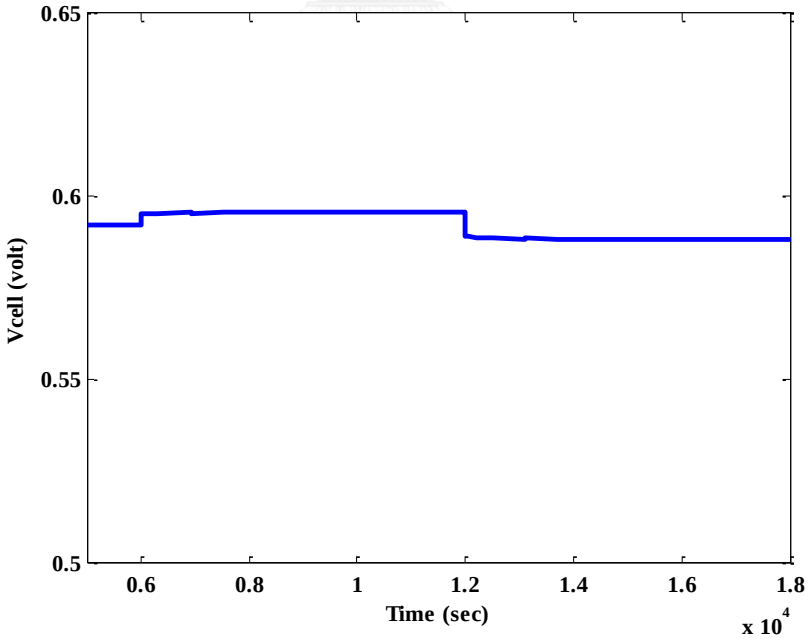

(b)

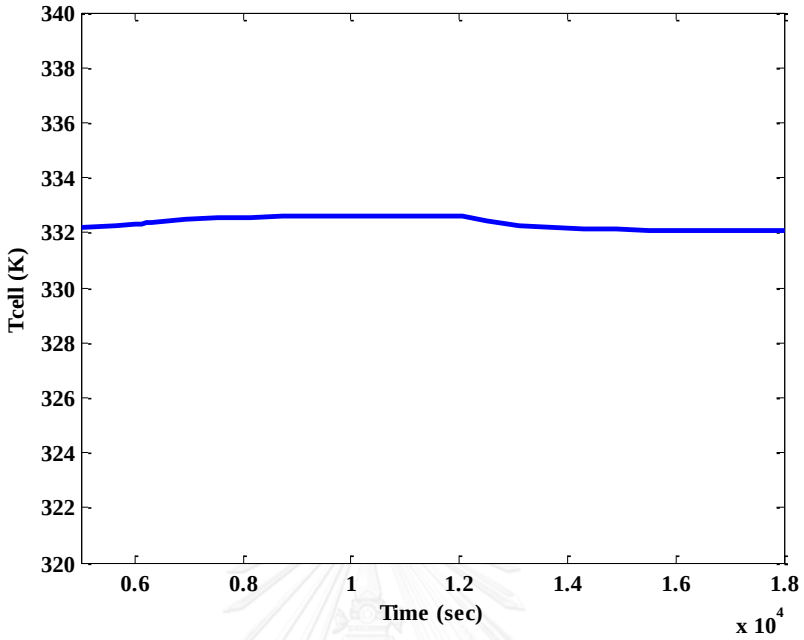

Figure 4.8 Transient responses as the inlet flow rate of hydrogen; (a) cell voltage, (b) cell temperature

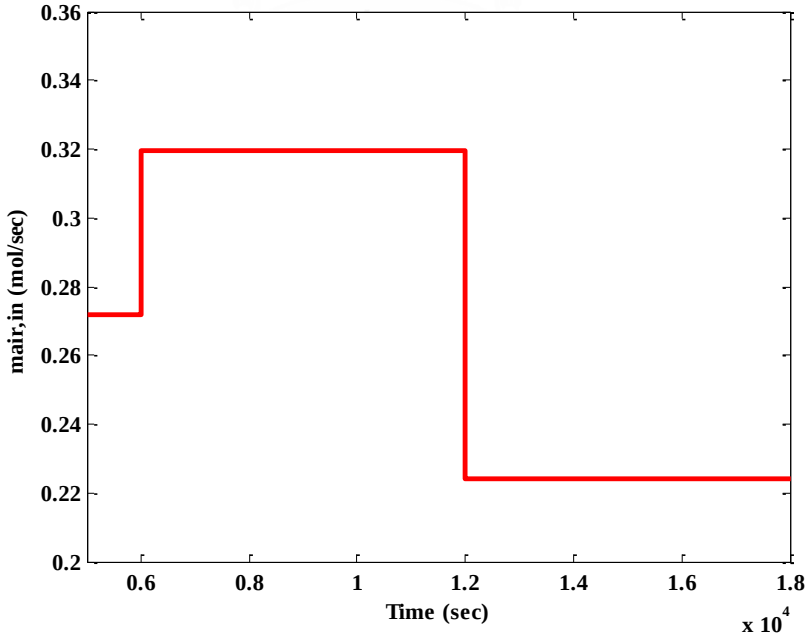

Figure 4.9 A step change in the inlet flow rate of air

(a)

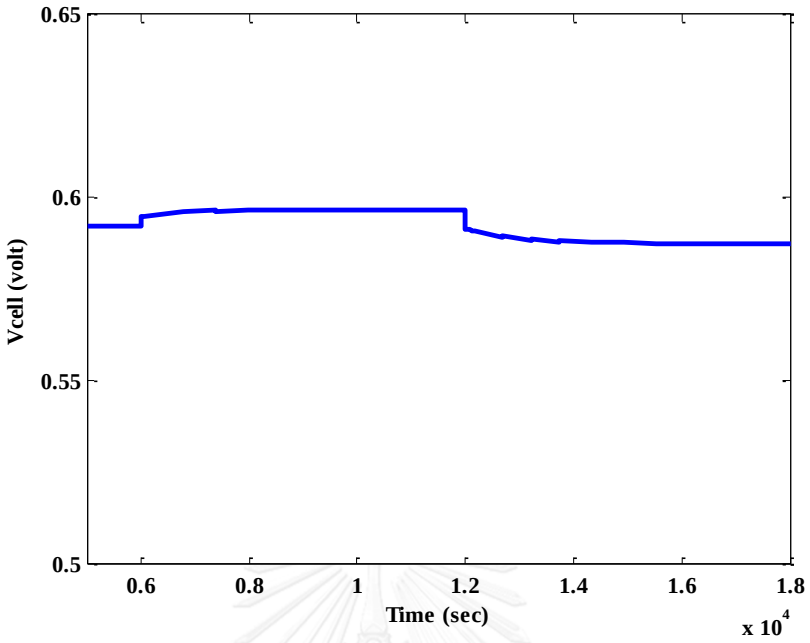

(b)

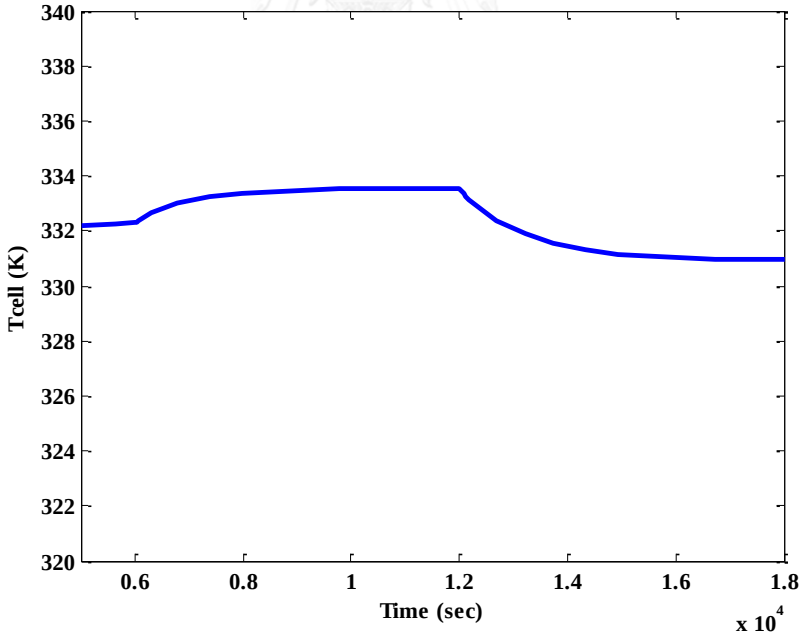

Figure 4.10 Transient responses as the inlet flow rate of air; (a) cell voltage, (b) cell temperature

4.4.3.3 Effect of a step change in temperatures of hydrogen and air

Figure 4.11 - 4.14 display the transient responses of the cell voltage and the cell temperature, when a step changes in the temperatures of hydrogen and air are increased from 348 K to 358 K at 6,000 sec, and then decrease from 358 K to 338 K at 12,000 sec. The results indicate that when the temperature of hydrogen is changed, an increase in the cell voltage and cell temperature have small responses but the cell outputs respond to the changes of the temperature of air. This shows that the cell voltage increases when the temperature of air increases because of decrease in the ohmic losses. Also, the cell temperature increases due to more heat enters into the fuel cell.

As mentioned above, the transient response of PEMFC in terms of the cell voltage and cell temperature are analyzed by using the step change in the operating conditions such as the inlet flow rates of hydrogen and air, the temperatures of hydrogen and air and the current density.

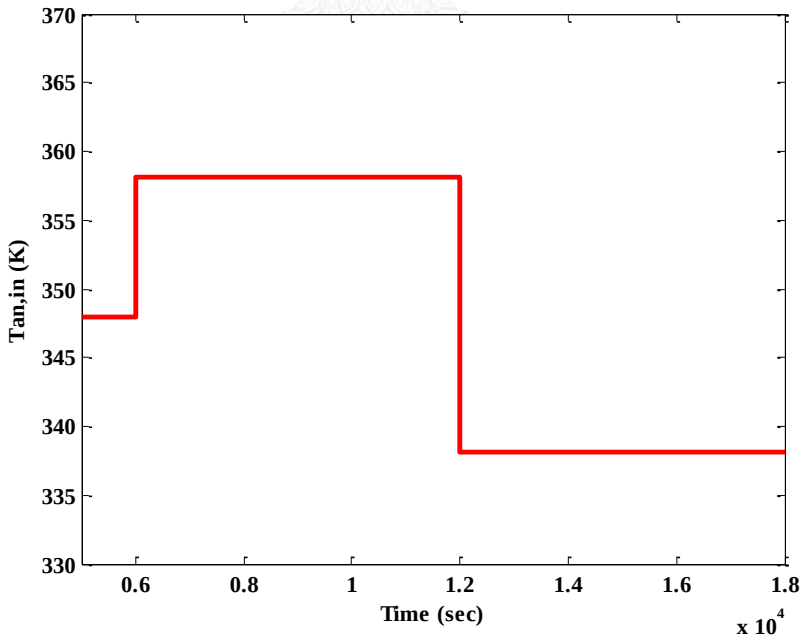

Figure 4.11 A step change in the temperature of hydrogen

(a)

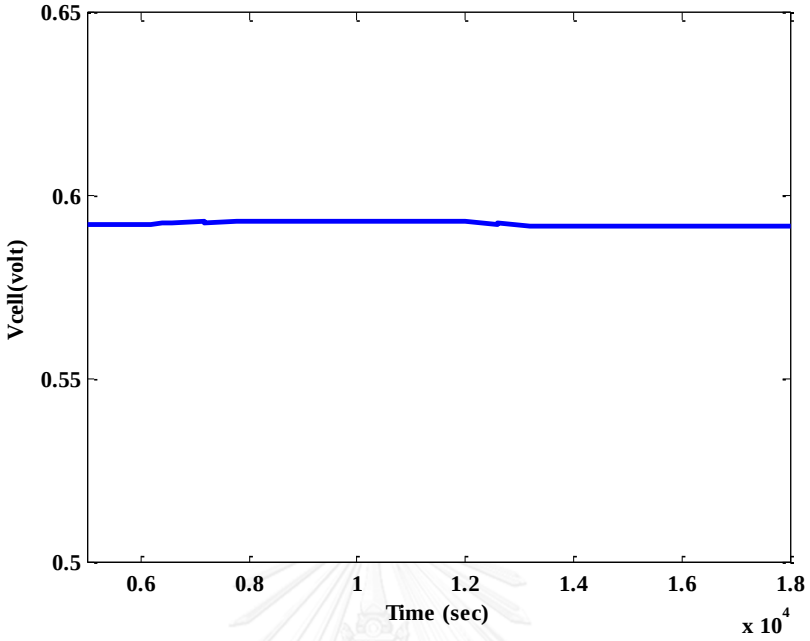

(b)

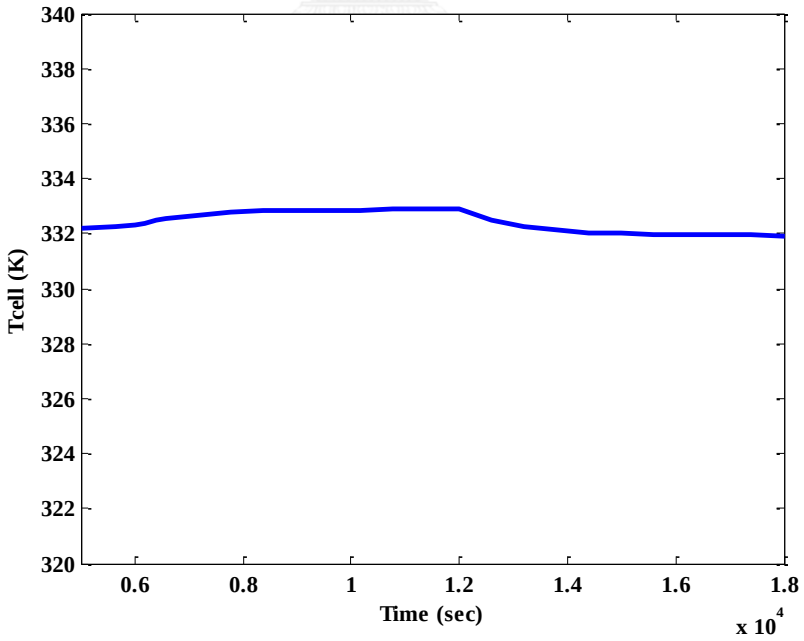

Figure 4.12 Transient responses as the temperature of hydrogen; (a) cell voltage, (b) cell temperature

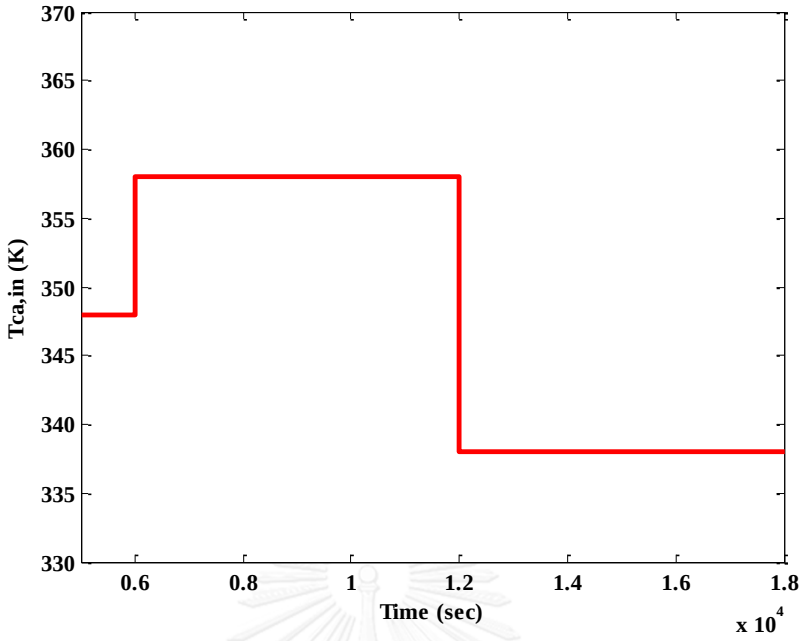

Figure 4.13 A step change in the temperature of air

(a)

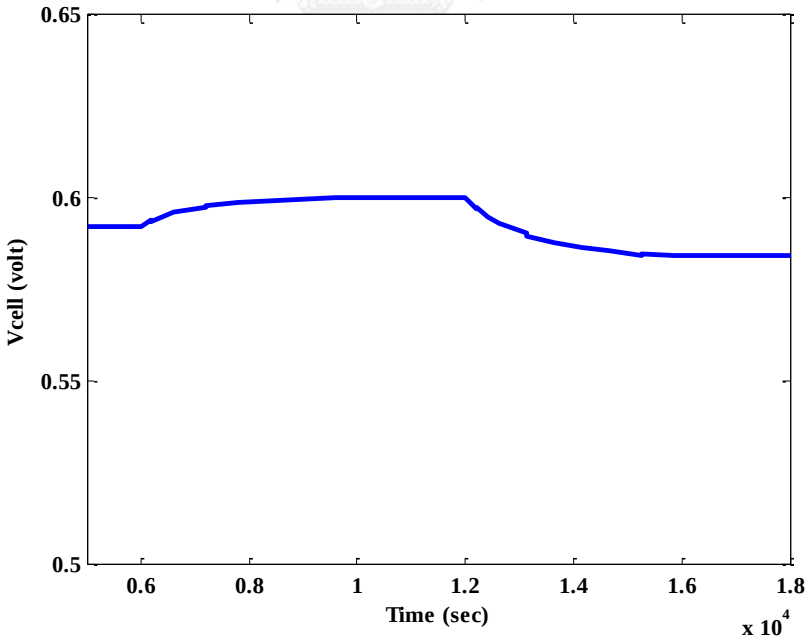

(b)

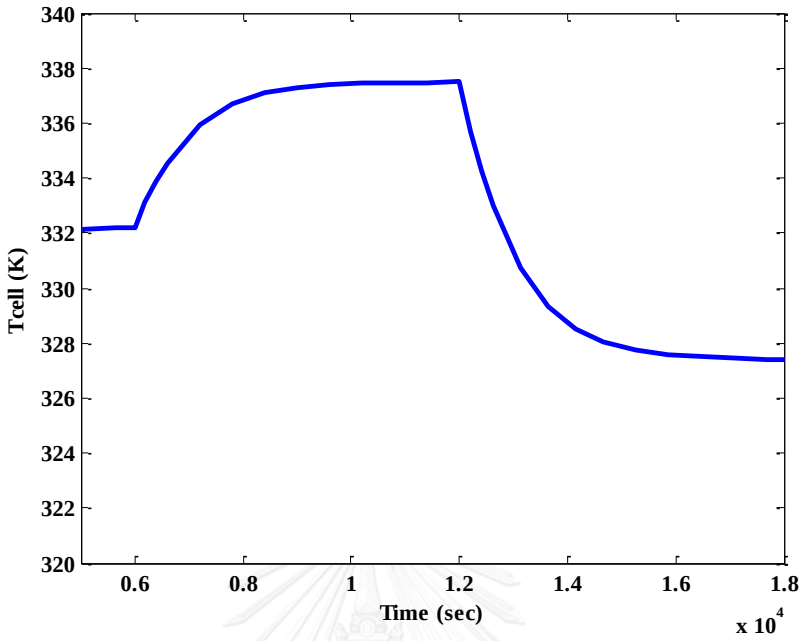

Figure 4. 14 Transient responses as the temperature of air; (a) cell voltage, (b) cell temperature

CHAPTER V

CONTROL OF A POLYMER EXCHANGE MEMBRANE FUEL CELL

5.1 Control Structure Design for PEMFC

A PEMFC is a multi-input-multi-output (MIMO) system. MIMO control problem is complex because there are many controlled and manipulated variables and process interaction among their variables. It may become poor performance control. The objective in this work is to maintain cell temperature, then another controlled variables is selected by fining a self-optimizing control structure for the controlled variables keep them constant at their set-points and leads to near optimal operation when disturbances appear within the system. In addition, an analysis of the steady-state relative gain array (RGA) is considered for pairing of the controlled and manipulated variables.

5.1.1 Selection of Controlled Variable using Self-Optimizing Control

As mentioned in Chapter 3, we apply the concept of self-optimizing control to alter the controlled variables for the PEMFC system, a flowsheet diagram of a PEMFC is represented in Figure 5.1. Following the stepwise procedure for the controlled variables for PEMFC.

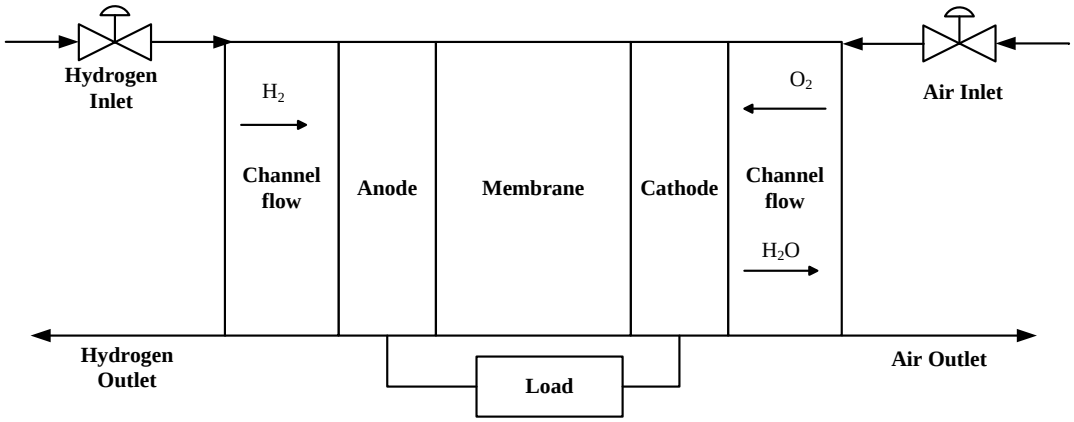

Figure 5.1 A flowsheet diagram of a PEMFC

Degree of freedom analysis.

At steady state, there are two operational degree of freedom; the inlet flow rates of hydrogen and air.

Definition of optimal operation

To specify the aim of operation, an economic cost function J is defined to minimize the cost of the hydrogen feed (m_{H_2}) minus the power value (P), subject to the constraints on the cell temperature kept constant at 332 K.

$$J = p_{H_2}\dot{m}_{H_2} - p_p P$$

where p_{H_2} denote the prices of the hydrogen flow rate ($/kg) and p_{H_2} represent the power density prices of the PEMFC for transportation application

Identification of important disturbances

The disturbances and process changes are considered in Table 5.1. The main disturbances are the current density and the temperatures of hydrogen and air.

Identification of candidate controlled variables

The cell temperature is active constraint, that is, it is optimal to have T_{cell} = 332 K. the following candidates for the controlled variable are considered three alternatives:

a. Partial pressure of hydrogen (p_{H_2})

b. Partial pressure of oxygen (p_{O_2})

c. Cell voltage (V_{cell})

Optimization.

An economic cost function J is defined to minimize the cost of the hydrogen feed minus the power value, subject to the constraints on the cell temperature kept constant at 332 K.

$$\min J = p_{H_2}\dot{m}_{H_2} - p_p P$$

Evaluation of loss for alternative combinations of controlled variables

To compare the options, the loss $L(u,d) = J(u,d) - J_{opt}(d)$ is calculated with each of the candidate variables kept constant at their nominal optimal value. The results of the loss for alternative controlled variables as given in Table 5.2 for the 3 candidate controlled variables and the 3 disturbances.

Final evaluation and selection

The following discussion to the results of the loss evaluation in Table 5.2, it is found that the partial pressure of hydrogen is selected the controlled variable because of the smallest economic loss. Moreover, the partial pressure of hydrogen is less sensitive to disturbances than the others as shown in Figure 5.2. It also responds to changes in the manipulated variable. Then, the partial pressure of hydrogen is suitable as the good controlled variable for control system.

Table 5.1 The disturbances

Disturbance	Normal value	Increase value	Decrease value
j (A/cm^2)	0.51	0.1	0.1
$T_{an,in}$ (K)	348	10	10
$T_{ca,in}$ (K)	348	10	10

Table 5.2 Loss evaluation for PEMFC

Disturbances \ Tasks				Optimal cost	Loss using constant p_{H2}	Loss using constant p_{O2}	Loss using constant V_{cell}
j	**T_{an}**	**T_{ca}**	**T_{cell}**				
0.51	348	348	332	-0.186052			
0.61	348	348	332	-0.223684	0.000131	0.000541	0.105060
0.41	348	348	332	-0.138561	0.000088	0.000396	0.112719
0.51	338	348	332	-0.18605	0.000109	0.000492	0.113822
0.51	358	348	332	-0.186054	0.000109	0.000492	0.113830
0.51	348	338	332	-0.186033	0.000110	0.000492	0.113809
0.51	348	358	332	-0.186074	0.000110	0.000492	0.113850

(a)

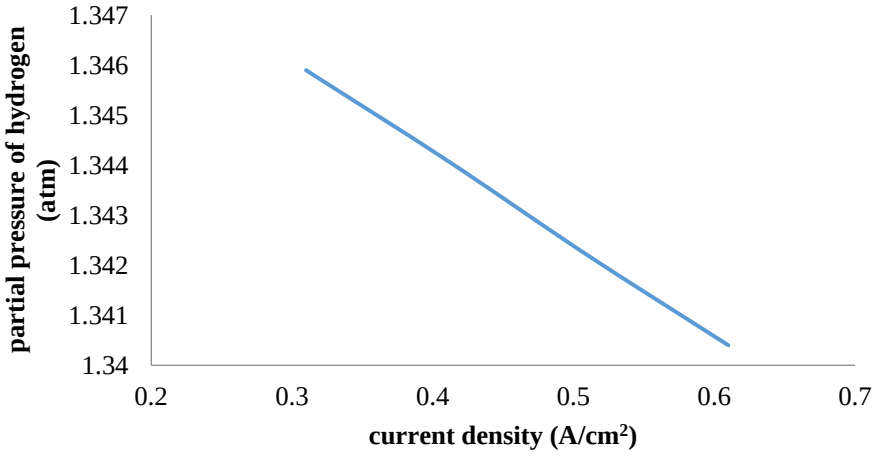

(b)

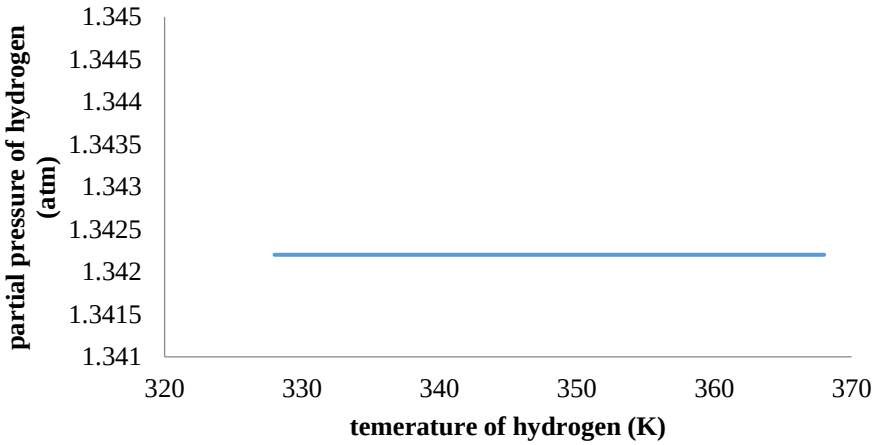

(c)

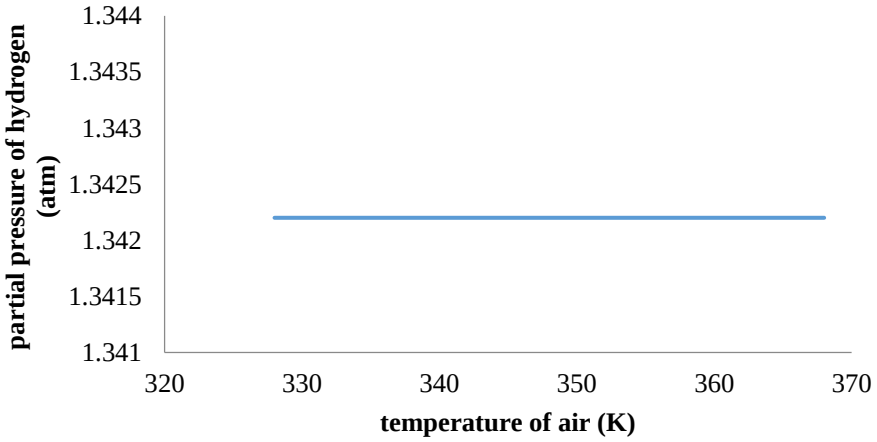

Figure 5.2 Relationships between partial pressure of hydrogen and disturbances; (a) current density, (b) temperature of hydrogen and (c) temperature of air

5.1.2 Pairing of Controlled and Manipulated Variable

A PEMFC is a multi-input-multi-output (MIMO) system. MIMO control problem is complex because there are many controlled and manipulated variables and process interaction among their variables. It leads to poor performance control. In general, changes in manipulated variables impact to all of controlled variables, therefore pairing of controlled and manipulated variable is important for minimizing interactions of PEMFC system. In this work, cell temperature and partial pressure of hydrogen as the controlled variables are needed to be regulated by manipulating inlet flow rates of hydrogen and air as the manipulated variables. Firstly, behavior of cell temperature and partial pressure of hydrogen are considered when inlet flow rates of hydrogen and air varies in range of operation. Figure 5.3-5.4 display relationships between cell temperature and partial pressure of hydrogen and inlet flow rate of hydrogen. When the inlet flow rate of hydrogen is increased, it can be seen that partial pressure of hydrogen immediately increased while cell temperature has less variation. Also, Figure 5.5-5.6 display relationships between cell temperature and partial pressure of hydrogen and inlet flow rate of air. When the inlet flow rate of air is increased, it can be seen that partial pressure of hydrogen keeps constant while cell temperature immediately increases. From the results, it is observed that cell temperature respond to change in inlet flow rate of air in air and partial pressure of hydrogen respond to change in inlet flow rate of hydrogen. Therefore, the cell temperature is controlled by manipulating inlet flow rate of air and partial pressure of hydrogen is controlled by manipulating inlet flow rate of hydrogen. To ensure these results, relative gain array (RGA) is used for pairing of controlled and manipulated variables.

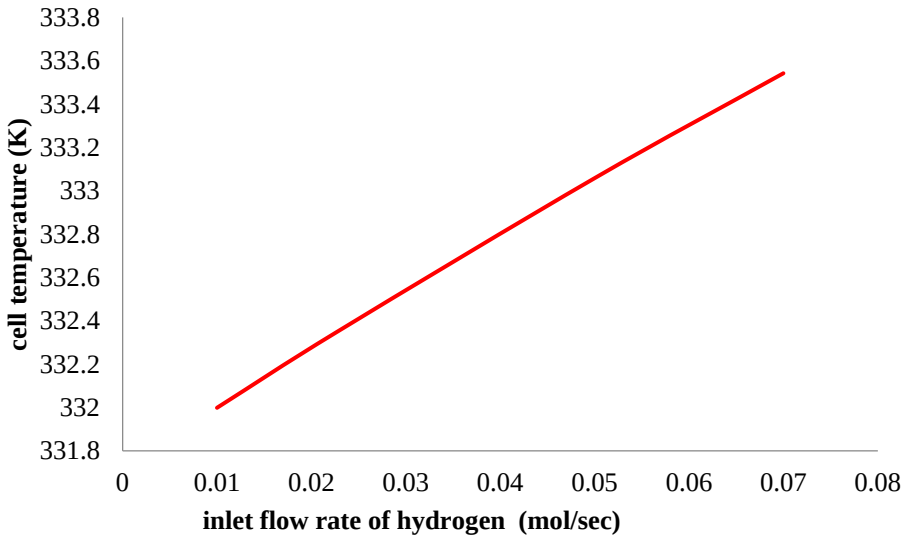

Figure 5.3 Relationships between cell temperature and inlet flow rate of hydrogen

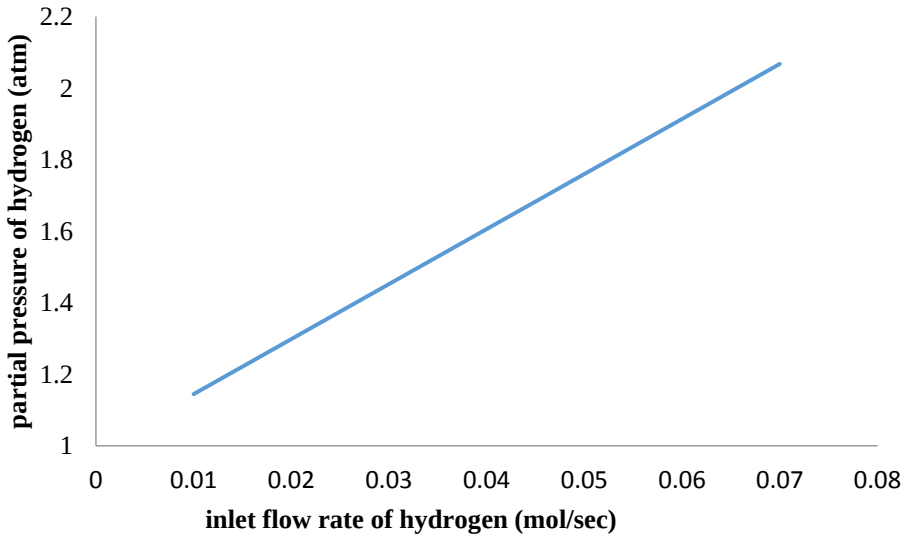

Figure 5.4 Relationships between partial pressure of hydrogen and inlet flow rate of hydrogen

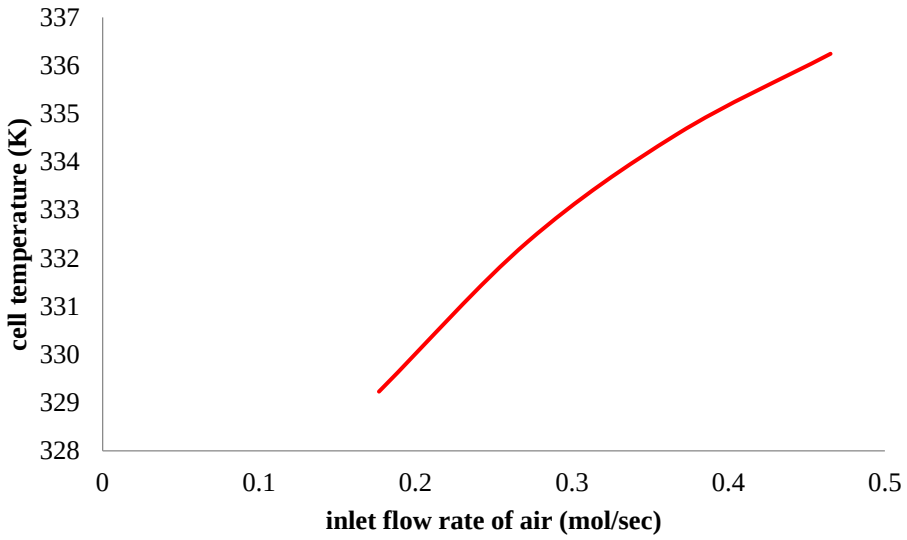

Figure 5.5 Relationships between cell temperature and inlet flow rate of air

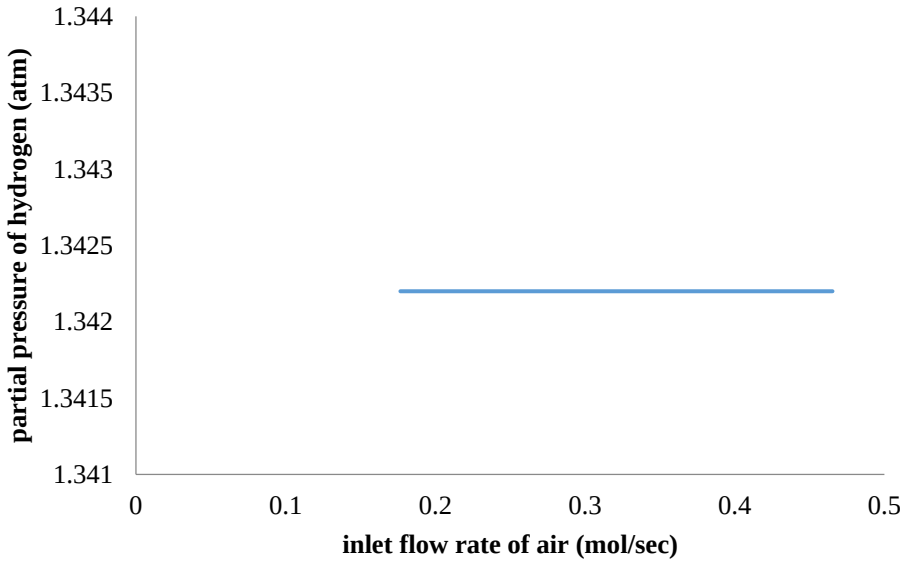

Figure 5.6 Relationships between partial pressure of oxygen and inlet flow rate of air

To get the best control performance for PEMFC, an analysis of the steady-state relative gain array (RGA) is considered. RGA is a form of the gain matrix that is used for selecting the optimal input-output variable pairings for a multi-input-multi-output (MIMO) system and describes the impact of each control variable on the output. The RGA of a non singular square complex matrix G is defined as

$$RGA = G * \ G^{-1\ T} \tag{5.1}$$

$$RGA = \begin{bmatrix} \lambda_{11} & \lambda_{12} \\ \lambda_{21} & \lambda_{22} \end{bmatrix} \tag{5.2}$$

where λ_{11} denote the relative gain between controlled variable y_1 and manipulated variable. Sum of each of row and column of array are equal to 1.

$$\lambda_{11} + \lambda_{12} = 1 \qquad \lambda_{11} + \lambda_{21} = 1 \tag{5.3}$$

$$\lambda_{21} + \lambda_{22} = 1 \qquad \lambda_{12} + \lambda_{22} = 1 \tag{5.4}$$

If $\lambda_{11} = 0$ means y_1 insensitive to u_1 and u_1 should not be pair with y_1. If $\lambda_{11} = 1$ means y_1 only sensitive to u_1 and does not interaction from u_2. If $0 < \lambda_{11} < 1$ means there are the amounts of interaction because not only y_1 will respond to u_1 but also u_2. G is the process gain matrix and is defined as

$$G = \begin{bmatrix} g_{11} & g_{12} & \cdots & g_{1n} \\ g_{21} & g_{22} & \cdots & g_{2n} \\ \vdots & \vdots & & \\ g_{n1} & g_{n2} & \cdots & g_{nn} \end{bmatrix} \tag{5.5}$$

Now that the steady state gain matrix has been determined, it is possible to use the RGA to compute the best manipulated variable control variable pairings. In this work, we consider the inlet flow rates of hydrogen (u_1) and air (u_2) as the input variables.

The cell temperature (y_1) and the partial pressure of hydrogen (y_2) are selected as the output variables. The first step is to calculate the steady state gain matrix. This gives an indication of the influence that each input has on each output.

$$G = \begin{bmatrix} 26.41 & 133.6 \\ 15.38 & 0 \end{bmatrix} \tag{5.6}$$

Then, the RGA can now be obtained according to this equation:

$$RGA = \begin{bmatrix} 0 & 1 \\ 1 & 0 \end{bmatrix} \tag{5.7}$$

The result of the RGA is 1 for the diagonal pairings (u_1-y_2, u_2-y_1). This implies that the partial pressure of hydrogen is controlled by using the inlet flow rate of hydrogen as manipulated variable. The cell temperature is controlled by using the inlet flow rate of air as manipulated variable. Consequently, the control structure of a PEMFC is shown in Figure 5.7.

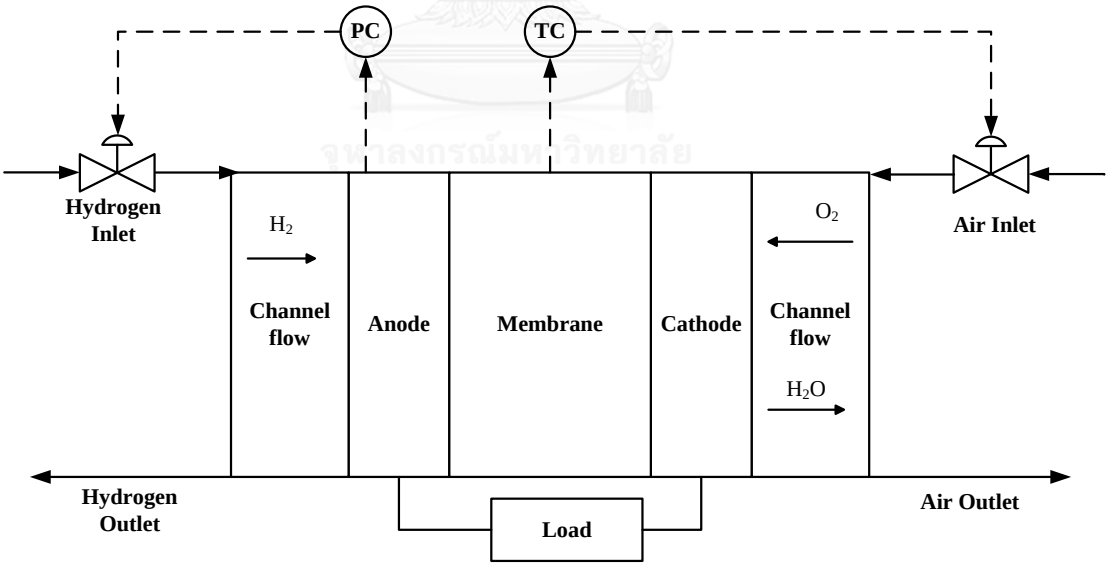

Figure 5.7 The control structure of a PEMFC

5.2 PI Controller Design

To regulate the cell temperature and partial pressure of hydrogen, in this work a proportional differential and integral (PI) controller is used because it is easy to implement and control a plant without information of the plant characteristics. The PI controller is the form of feedback control structure. The concept is to calculation of the manipulated variable (MV) by minimizing the error between the measured variable and the desired set-point. The general form of the PI algorithm is represented by:

$$u(t) = u_0 + K_c\left(e(t) + \frac{1}{\tau_I}\int_0^t e(\tau)\,d\tau\right) \tag{5.8}$$

where

K_c is proportional gain

τ_I is integral gain

e is error

t is time

τ is variation of integration

When the characteristics of a continuous process move away from steady state condition, their responses track to its set-point slowly. Therefore, three parameters K_c and τ_I must be adjusted in the PI controller for guaranteeing stability and performance which it is important to alter a suitable parameter for tuning PI controller. The increasing proportional term shows that the response of system is fast. If the proportional gain is too high, the response will come to be overshoot or unstable. If the proportional gain is too low, the control action is small when disturbance occur within system. For the integral term, the control action is to reduce steady state error and get rid of offset by decreasing value of the integral gain.

In this work, the SIMC (Skogested IMC) PI tuning rules are applied for PEMFC. The second-order time delay model for PI control is formulated in form *g(s)*

$$g(s) = \frac{k}{(\tau_1 + 1)(\tau_2 + 1)} e^{-\theta s} \tag{5.9}$$

where k represents the plant gain $(k = \Delta y(\infty) / \Delta u)$, τ_1 represents the time constant, τ_2 represents the second-order lag time constant and θ represents the times delay without output changes. The SIMC PI tuning rules for the second-order lag time delay process in eq. (5.9) are expressed as:

$$K_c = \frac{1}{k} \frac{\tau_1}{\tau_c + \theta} \tag{5.10}$$

$$\tau_1 = min\{\tau_1, 4(\tau_c + \theta)\} \tag{5.11}$$

$$\tau_D = \tau_2 \tag{5.12}$$

where τ_c is the closed-loop response time constant and $\tau_2 > \theta$ for dominant second-order process. For tuning parameter selection, τ_c is calculated between tight control that is the smooth control and good robustness.

- Simulation Results when disturbance changes for PI controller

As a mentioned in a previous section, since PEMFC is a MIMO dynamic nonlinear system, the RGA analysis recommends that not only the molar flow rate of air can be manipulated variable to control the cell temperature but also molar flow rate of hydrogen can be manipulated variable to control the partial pressure of hydrogen. Therefore, two PI control loops are adopted to control the PEMFC operation under the variation of current density as disturbance. The control scheme for PEMFC system is shown in Figure 5.7. The first loop is designed by using the first PI controller with the molar flow rate of air as manipulated variable to maintain the cell temperature whereas the second loop is designed by using another PI controller with the molar flow rate of hydrogen as manipulated variable to regulate partial pressure of hydrogen. The PI tuning parameters are shown in Table 5.3.

Table 5.3 The PI tuning parameters of the cell temperature and partial pressure of hydrogen control loops

Controller parameter	Cell temperature	Partial pressure of hydrogen
K_c	1	0.015
τ_I	10	2

The disturbance as current density is varied for testing the transient behaviors of PEMFC system. Figure 5.8(a) shows the variation of current density step changes from 0.511 to 0.515, and 0.507 A/cm^2 at times t = 100, 1,500 sec, respectively. The closed-loop responses of the PEMFC are shown in Figures 5.8(b) to 5.8(c).

After the current density change from 0.51 A/cm^2 to 0.515 A/cm^2 at the instant time 300 sec. It is obvious that the cell temperature raises a transient response up and backs to a steady state response since the molar flow rate of air is adjusted under the disturbances as shown in Figure 5.8(b). Moreover, the variation of the partial pressure of hydrogen decreases because the hydrogen consumption is high with increasing current density, hence the PI controller speeds up hydrogen flow rate in order to compensate the level of hydrogen consumption as shown in Figure 5.8(c)

(a)

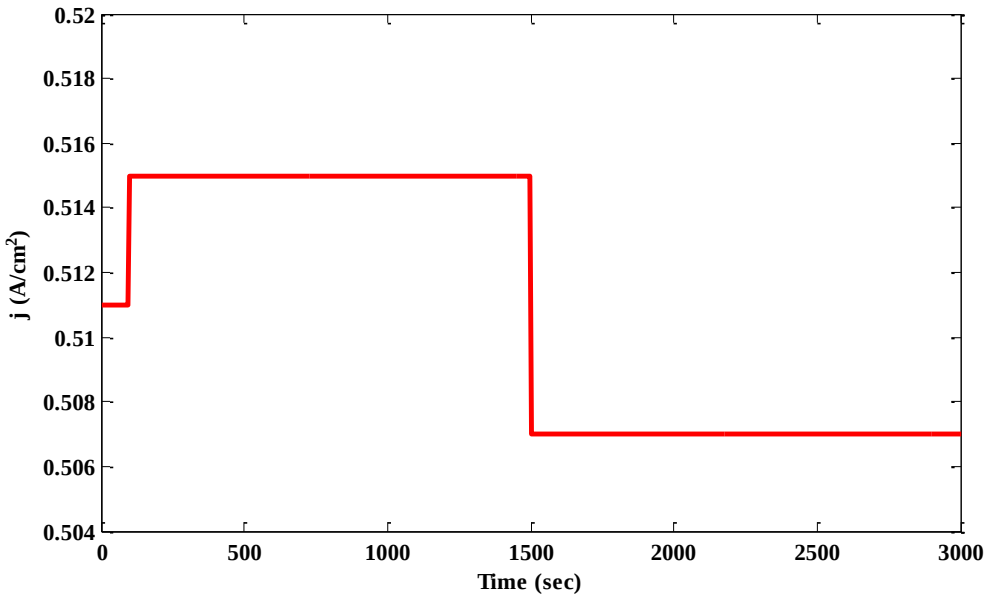

(b)

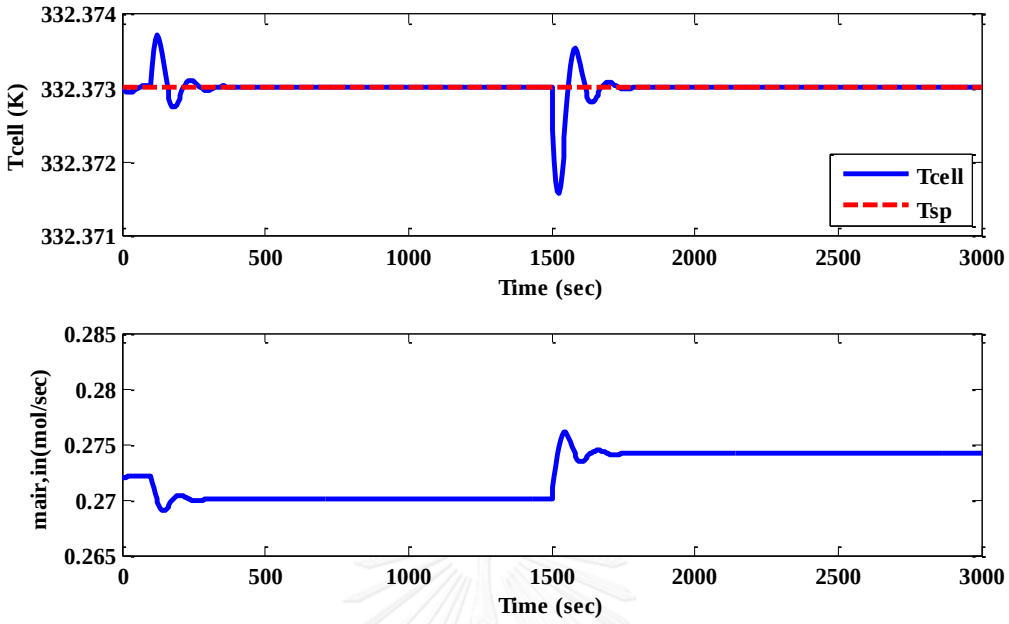

(c)

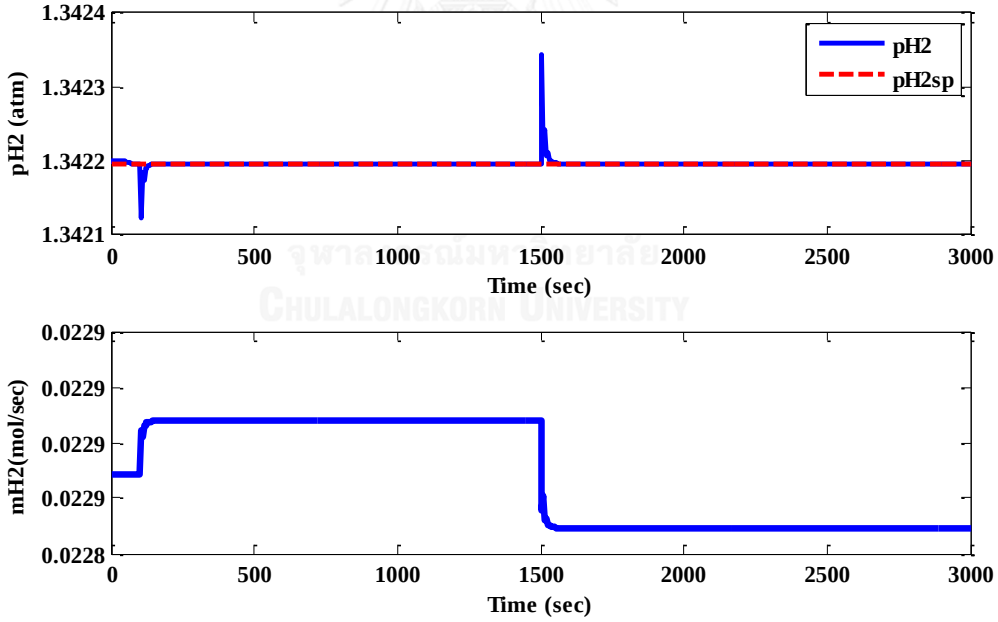

Figure 5.8 Performance of PI controller: (a) step current density; (b) response of cell temperature using the inlet flow rate of air as manipulated variable; (c) response of partial pressure of hydrogen using the inlet flow rate of hydrogen as manipulate variable

5.3 MPC Controller Design and Setup

In this work, we use the model predictive control toolbox in MATLAB for control of a PEMFC. The MPC toolbox requires the linear model, time invariant (LTI). Hence, the nonlinear dynamic model of a PEMFC must be convert to linear time-invariant system. In addition, we must specify the characteristics of each plant model input and output signal and the characteristics of measured and unmeasured disturbances. In the case study, we omit the measurement noise and the additive integrated white noise on each measured output. Then, the horizon and weights are specified. The control interval (sampling time) is 5 sec. The prediction horizon is set to 10 samples and the control horizon 2 samples. The manipulated variable are the inlet flow rates of air and hydrogen. The outputs are cell temperature and partial pressure of hydrogen to be regulated at their set-points. The outputs are equally weighted while the input weights are the same value. Finally, input and output constraints are defined. The inlet flow rate of air is bound between 0.01 mol/sec and 0.10 mol/sec the inlet flow rate of hydrogen is bound between 0.01 mol/sec and 0.10 mol/sec. All outputs are unconstrained.

5.4 Robust MPC Design and Setup

In this section the implementation of the ellipsoidal off-line robust MPC algorithm for linear time variant (LTV) of the PEMFC is evaluated by using polytopic system. The optimization has been computed using YALMIP (Löfberg, 2004) and solver SeDuMi (Sturm 1988) within the MATLAB environment (R2012a).

Consider the nonlinear model of a PEMFC system. The cell voltage is considered to be the uncertain parameter. The linearized mathematical model of PEMFC based on the mass and energy balances is derived under the assumption that the control inputs, u are the inlet flow rates of hydrogen and air, and current density. The state variables, x are the cell temperature and the partial pressure of hydrogen. y is the output variable. Then, the considered continuous linearized model of the PEMFC is in the form:

$$\begin{aligned} \dot{x} &= Ax + Bu \\ y &= Cx \end{aligned} \tag{5.13}$$

where $A=\begin{bmatrix} a_{11} & a_{12} & a_{13} \\ a_{21} & a_{22} & a_{23} \\ a_{31} & a_{32} & a_{33} \end{bmatrix}$, *and* $B=\begin{bmatrix} b_{11} & b_{12} \\ b_{21} & b_{22} \\ b_{31} & b_{32} \end{bmatrix}$

To obtain the discrete-time model of the PEMFC by using Euler first-order approximation with a sampling time of 5 s. Therefore, we define $\bar{x}=x-x_{ss}, \bar{u}=u-u_{ss}$ where subscript ss is used to denote the corresponding variable at steady state condition.

$$\begin{aligned} \bar{x}(k+1) &= A\bar{x}(k)+B\bar{u}(k) \\ \bar{y}(k) &= C\bar{x}(k) \end{aligned} \tag{5.14}$$

where $A=\begin{bmatrix} a_{11}\Delta t+1 & a_{12}\Delta t & a_{13}\Delta t \\ a_{21}\Delta t & a_{22}\Delta t+1 & a_{23}\Delta t \\ a_{31}\Delta t & a_{32}\Delta t & a_{33}\Delta t+1 \end{bmatrix}$, *and* $B=\begin{bmatrix} b_{11}\Delta t & b_{12}\Delta t \\ b_{21}\Delta t & b_{22}\Delta t \\ b_{31}\Delta t & b_{32}\Delta t \end{bmatrix}$

Since there is one uncertain parameter as the cell voltage that is varied between 0.55 V and 0.65 V, the polytopic uncertain model is considered with the two different vertices system describing behavior of a PEMFC. The polytopic uncertainty is described as follows:

$$B \in \Omega = Co\{B_1, B_2\} \tag{5.15}$$

The objective is to regulate the state variables to the origin by manipulating the control inputs. The cost function $J_{\infty}(k)$ is expressed by

$$J_{\infty}(k)=\sum_{i=0}^{\infty}[x(k+i|k)^T \Theta x(k+i|k)+u(k+i|k)^T Ru(k+i|k)] \tag{5.16}$$

with $\Theta = I, R = 0.1I$

- Comparisons of PI, MPC and robust MPC controllers

In this PI controller design, Figure 5.10 (a) and 5.11 (a) display the closed-loop response the regulated outputs and Figure 5.12 displays the control inputs of PI controller. It can be seen from Figure 5.9 (a) that the PI controller is able to track the set-point value when initial value of the cell temperature is raised up to 10 K. Although there is a small oscillation in the regulated outputs, the cell temperature can reach the set-point value within 10,000 sec. The cell voltage can also track to the desire value as shown in Figure 5.15 (a).

In this MPC controller design, Figure 5.10 (b) and 5.11 (b) display the closed-loop response the regulated outputs and Figure 5.13 displays the control inputs. It can be seen from Figure 5.9 (b) that the MPC controller is able to track the set-point value when initial value of the cell temperature is raised up to 10 K. Although there is a small oscillation in the regulated outputs, the cell temperature can reach the set-point value within 1,000 sec. The cell voltage can also track to the desire value as shown in Figure 5.15 (b).

In this robust MPC controller design, one uncertain parameter as the cell voltage is randomly time-varying between 0.55 V and 0.65 V. Figure 5.10 and 5.11 display the regulated outputs and Figure 5.14 displays the control inputs. The simulation results reveal that a robust MPC algorithm using ellipsoidal invariant can maintain the regulated outputs by manipulating the control inputs to their set-points. Clearly, all of the state variables approach their set-point quickly that are less than 20 sec while constraints on inputs are satisfied. The cell voltage can track to the desire value as shown in Figure 5.15 (c). It means that also guarantee performance of a PEMFC system. Moreover, it can be observed that an off-line robust MPC algorithm using ellipsoidal invariant can achieve better control performance than PI and MPC controller because an off-line robust MPC can guarantee robust stability.

(a)

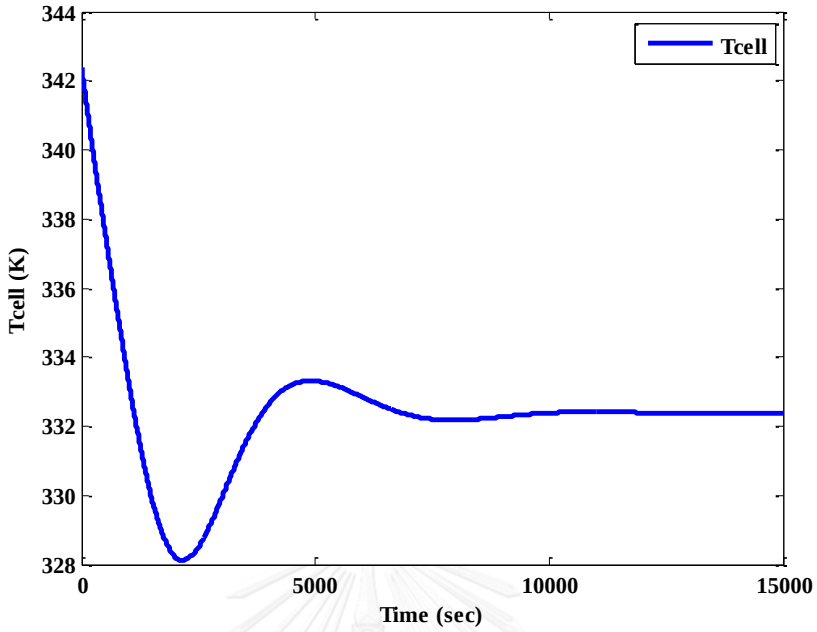
Tcell
344
342
340
338
336
334
332
330
328
Tcell (K)
0
5000
10000
15000
Time (sec)

(b)

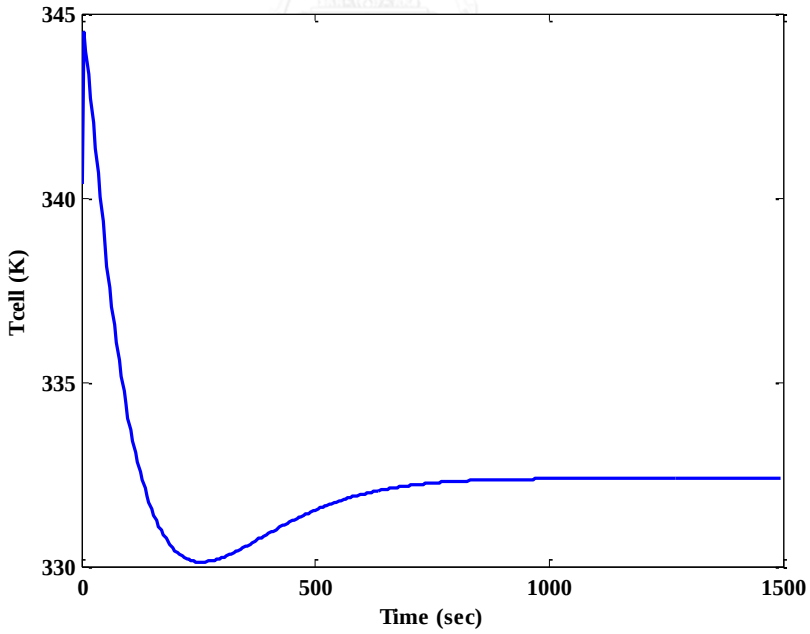
345
340
335
330
Tcell (K)
0
500
1000
1500
Time (sec)

(c)

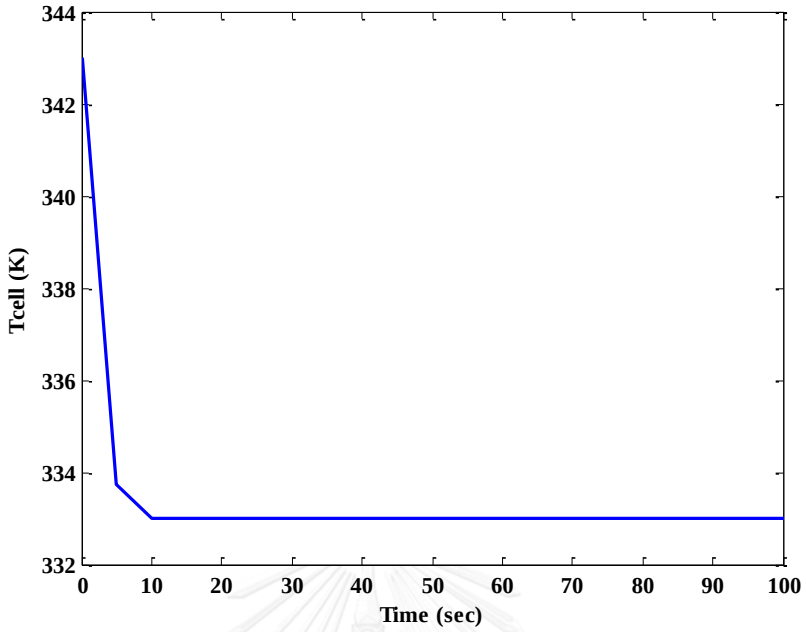

Figure 5.9 The closed-loop responses of PEMFC temperature: (a) PI controller; (b) MPC controller; (c) robust MPC controller

(a)

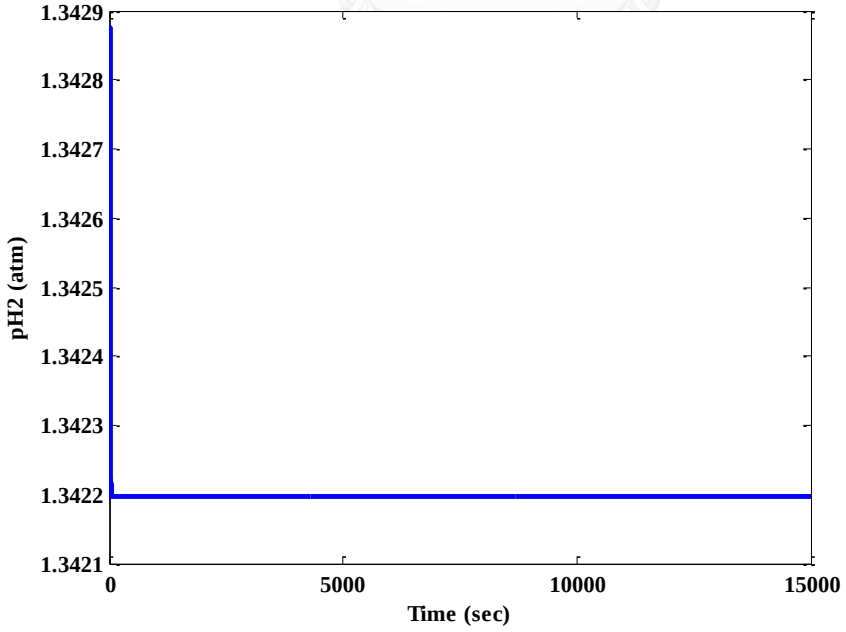

(b)

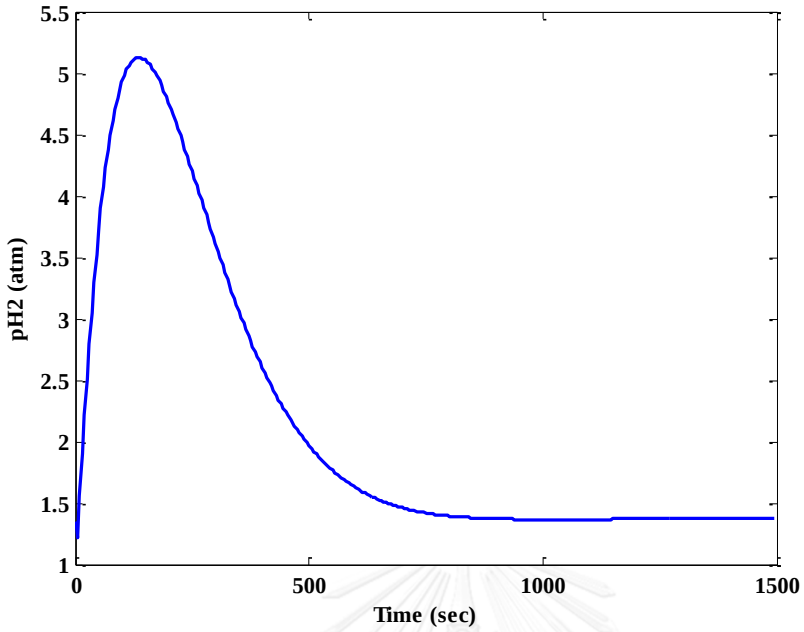

(c)

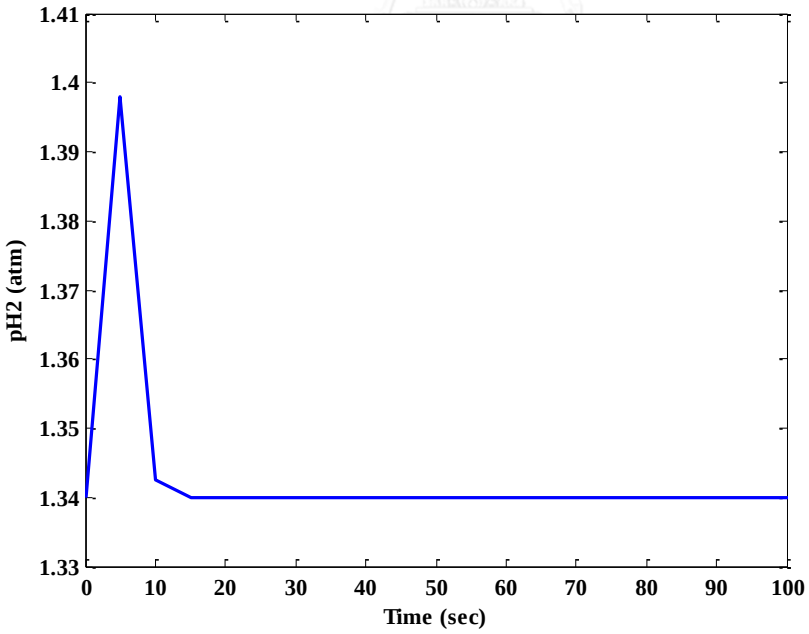

Figure 5.10 The regular output in term partial pressure of hydrogen: (a) PI controller; (b) MPC controller; (c) robust MPC controller

(a)

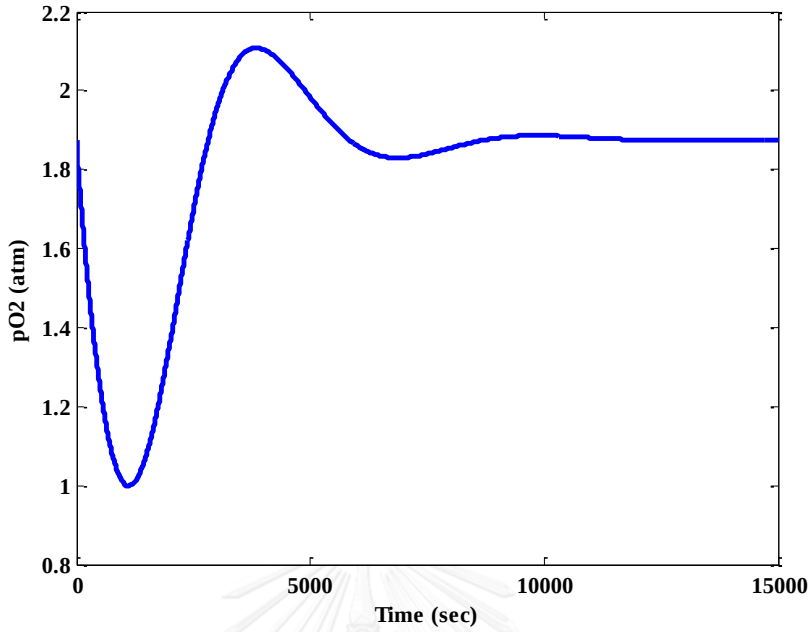
2.2
2
1.8
1.6
1.4
1.2
1
0.8
pO2 (atm)
0
5000
10000
15000
Time (sec)

(b)

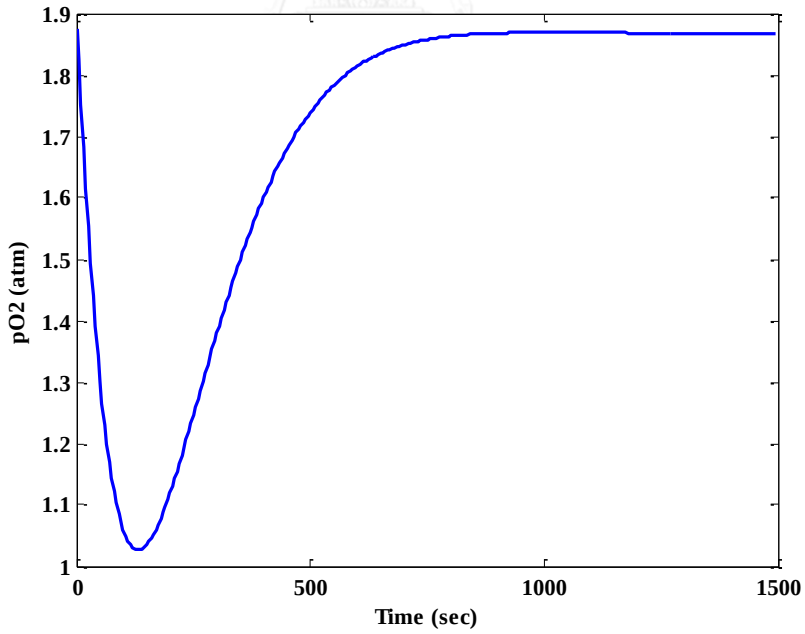
1.9
1.8
1.7
1.6
1.5
1.4
1.3
1.2
1.1
1
pO2 (atm)
0
500
1000
1500
Time (sec)

(c)

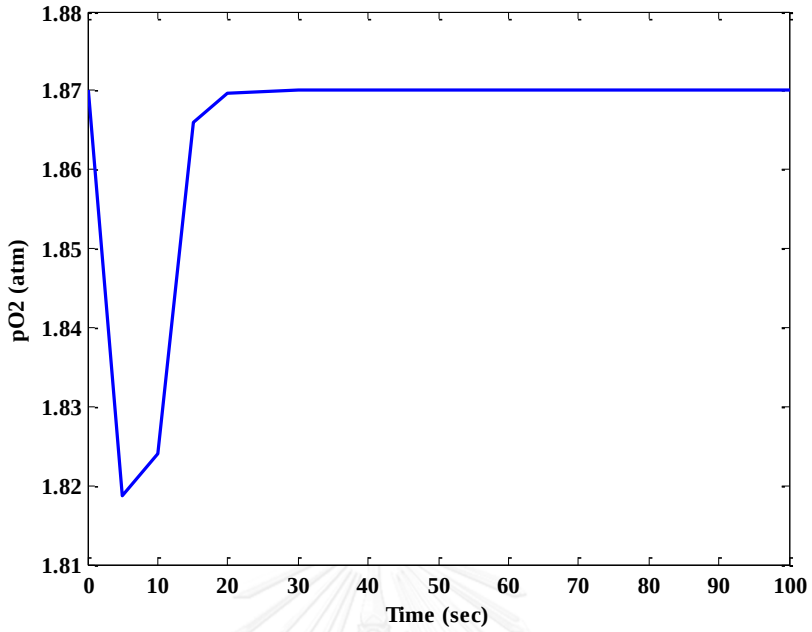

Figure 5.11 The regular output in term partial pressure of oxygen: (a) PI controller; (b) MPC controller; (c) robust MPC controller

(a)

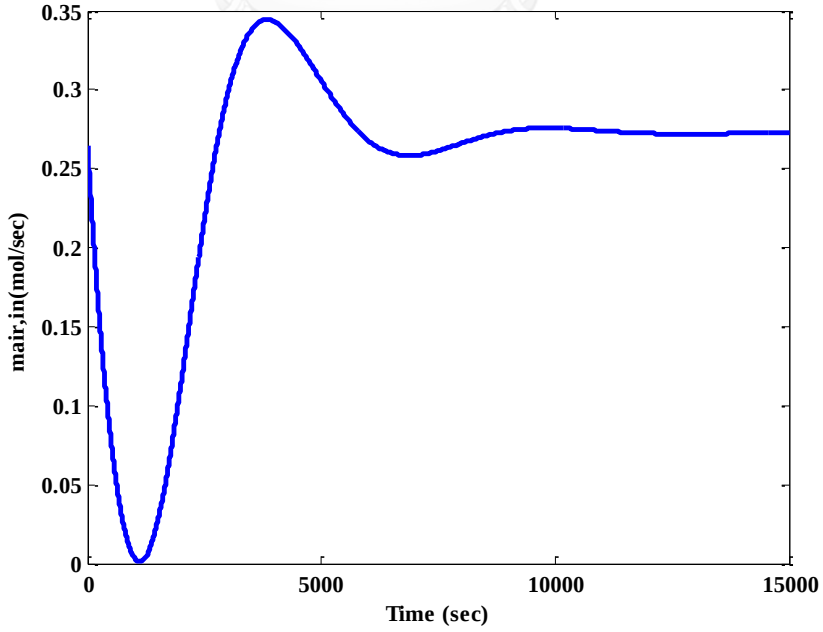

(b)

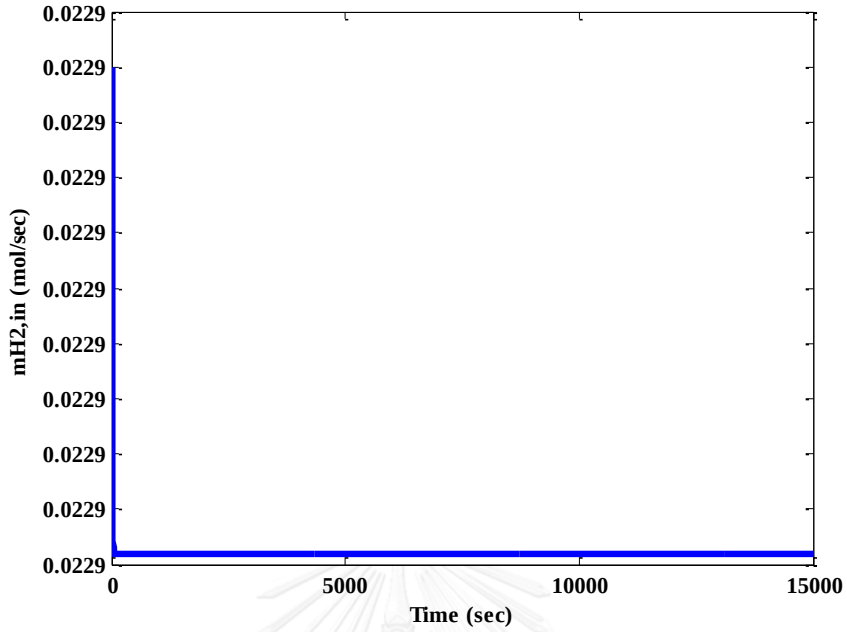

Figure 5.12 The control inputs of PI controller: (a) inlet flow rate of air; (b) inlet flow rate of hydrogen

(a)

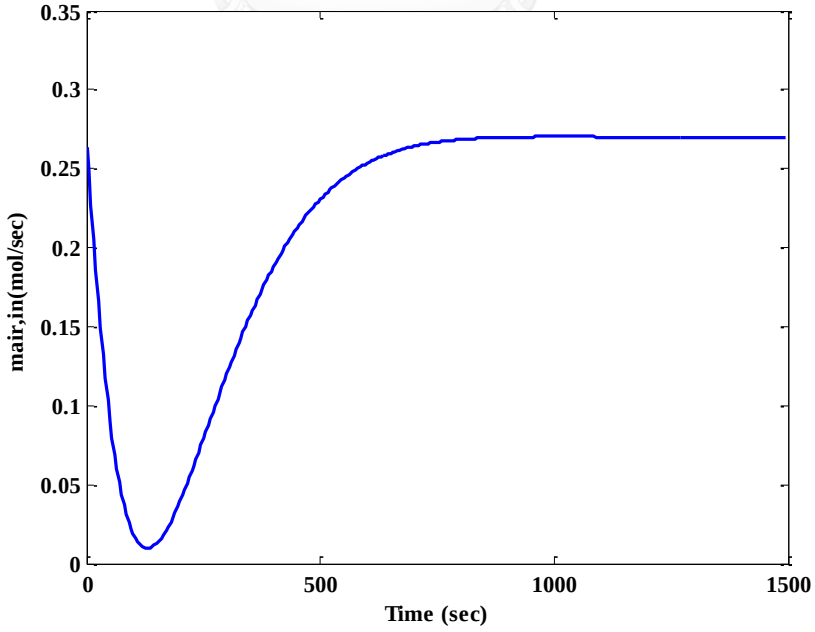

(b)

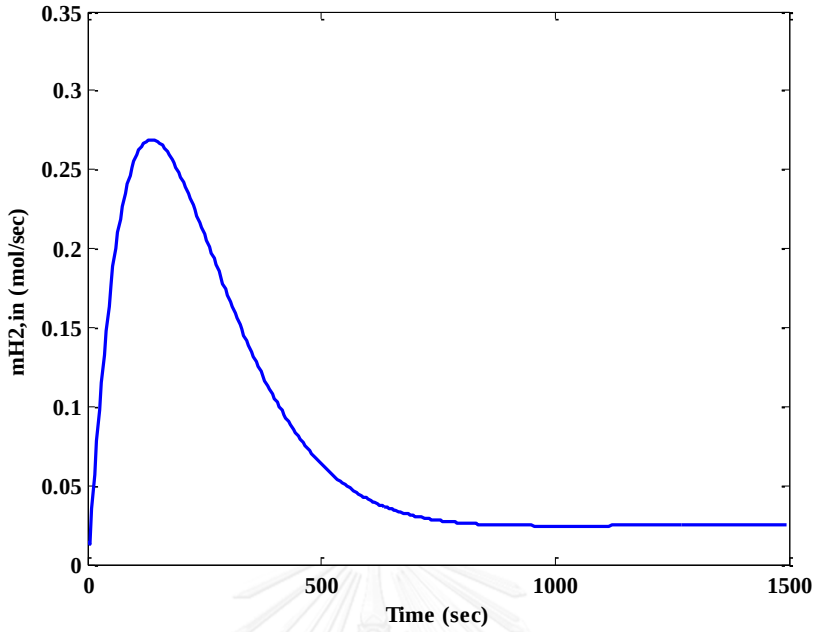

Figure 5.13 The control inputs of MPC controller: (a) inlet flow rate of air; (b) inlet flow rate of hydrogen

(a)

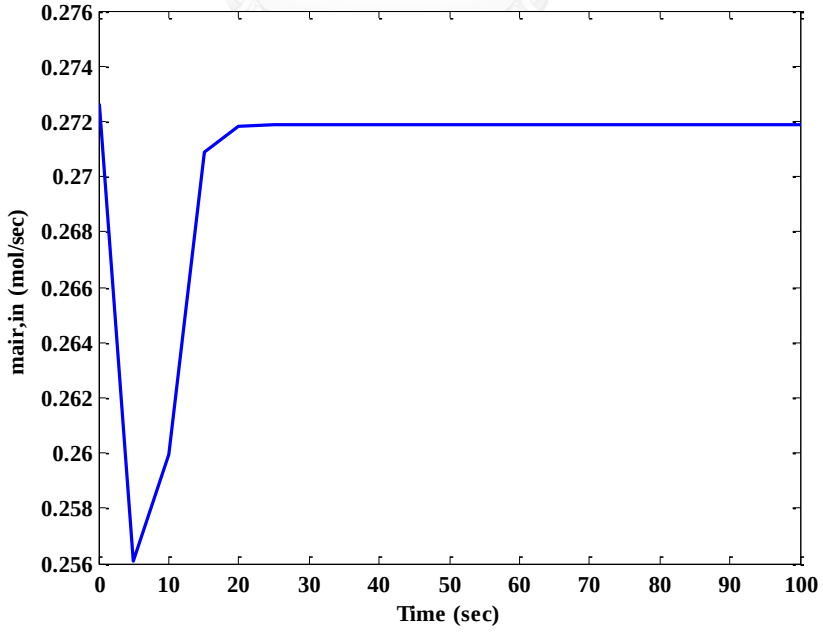

(b)

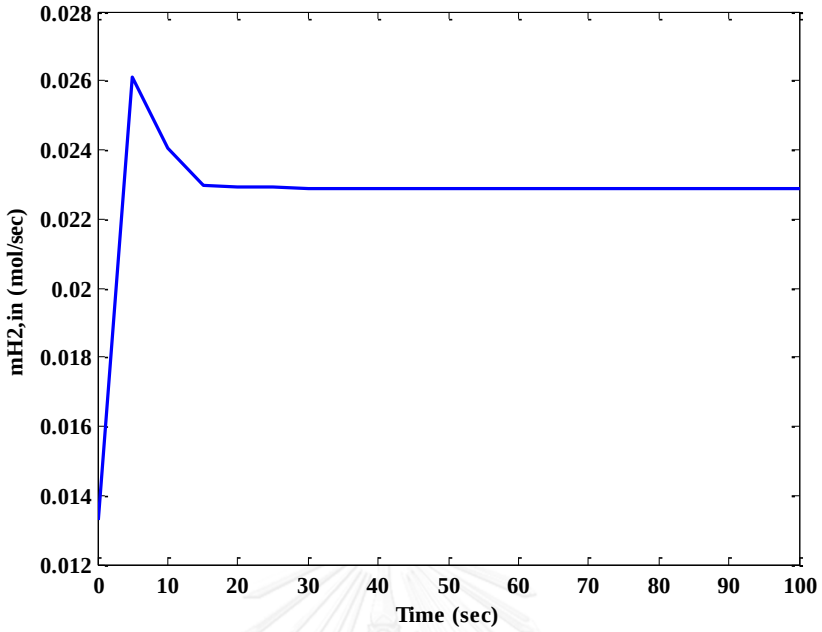

Figure 5.14 The control inputs of robust MPC controller: (a) inlet flow rate of air; (b) inlet flow rate of hydrogen

(a)

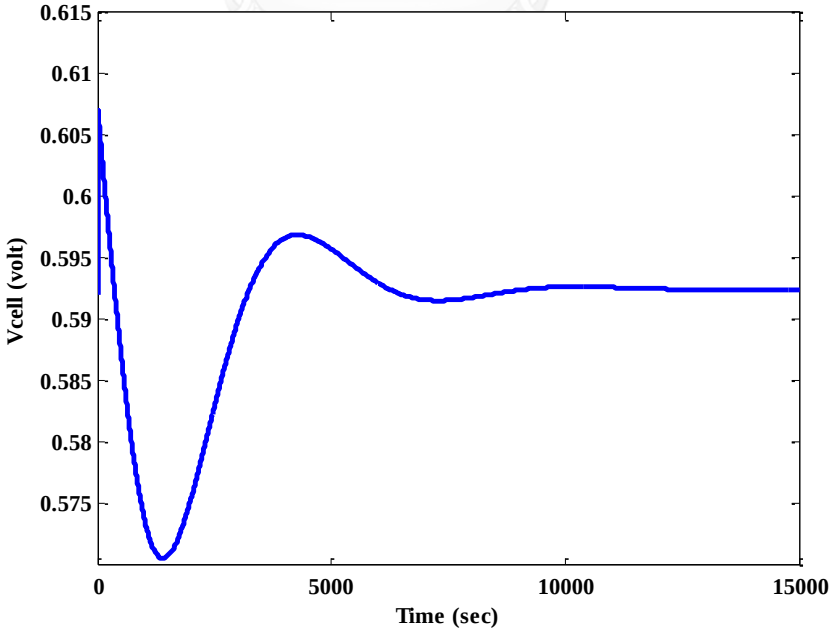

(b)

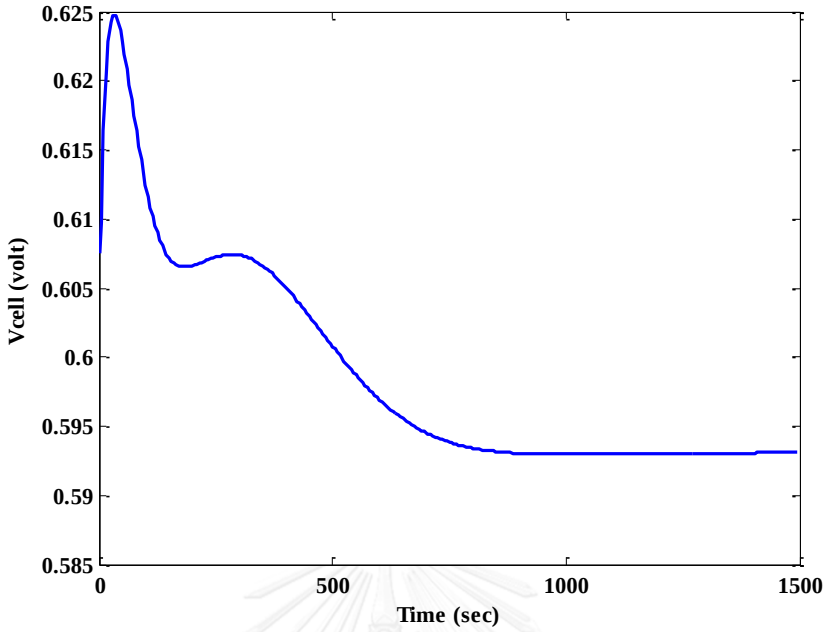

(c)

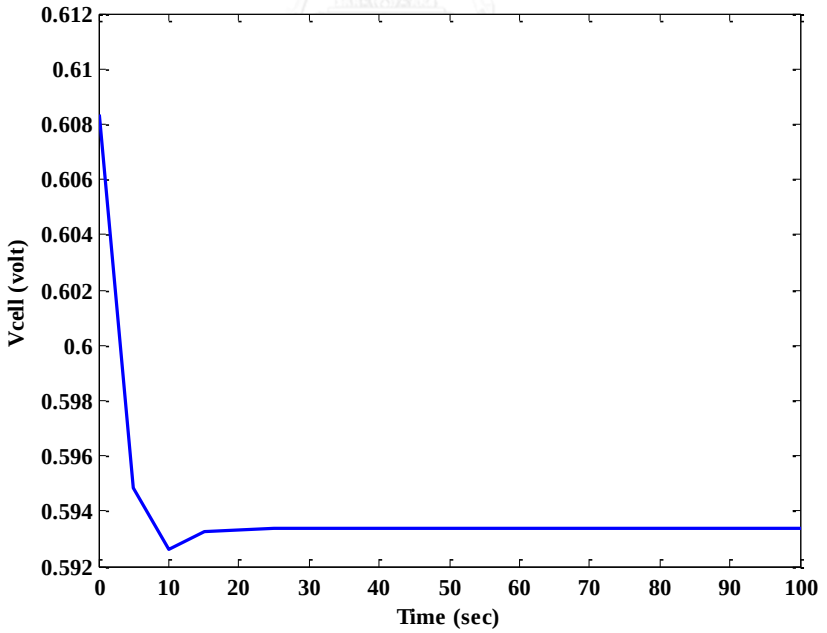

Figure 5.15 Response of cell voltage; (a) PI controller, (b) MPC controller, (c) robust MPC controller

CHAPTER VI
CONCLUSIONS AND RECOMMENDATIONS

6.1 Conclusions

In this study, the PEMFC fed by pure hydrogen and air is considered. Lumped dynamic model is used, includes mass balances for the anode and cathode side and energy balance for the fuel cell. The transient behaviors of the PEMFC are investigated under various operating conditions. Moreover, the selection of the controlled variable for system is considered by using a self-optimizing control approach where fixing the primary controlled variable is constant at its set-point lead to near-optimal operation. The performance of PI controller is implement for the PEMFC system. Moreover, the performance of robust model predictive control (robust MPC) is evaluated the PEMFC system and compared with the model predictive control (MPC).

The study is performed on a nonlinear dynamic model of a PEMFC. It is a lumped model that describes quite well the system dynamics. The MATLAB solver is used to implement the dynamic simulation of a PEMFC. To ensure the PEMFC model can reliably predict the performance of the PEMFC, the simulated polarization curve is compared with the experimental data reported in the literature. Most of the simulation results were good agreement with the literature and this confirm that the dynamic model was developed in this study is reliable. Next, the dynamic responses of the cell voltage and cell temperature are discussed. Dynamic behavior is especially the most significant for fuel cell operation that should be studied under operating conditions such as temperature, flow rate of the reactant gases etc. Therefore, it is necessary to study the dynamic behavior of the PEMFC to investigate the responses of the cell voltage and cell temperature and to achieve stable performance under various operating conditions such as variation of current density, inlet flow rates of hydrogen and air, and temperatures of hydrogen and air.

Control Structure Design for PEMFC is investigated. The objective is to find the good controlled variables is selected by finding a self-optimizing control structure for the controlled variables keep them constant at their set-points and leads to near optimal operation when disturbances appear within the system. To accomplish the

controlled variable, we evaluate the steady state economic loss (L) as the difference between the actual value of a given cost function and the truly optimal value of the cost function. We specify the cell temperature as active constraint. The candidate controlled variables are cell voltage, partial pressures of hydrogen and oxygen. The result was found that the partial pressure of hydrogen is selected to be the controlled variable because of the smallest economic loss. Moreover, the partial pressure of hydrogen is less sensitive to disturbances than the others. In addition, an analysis of the steady-state relative gain array (RGA) is considered for pairing of the controlled and manipulated variables. The result of the RGA was 1. This implies that the partial pressure of hydrogen is controlled by using the inlet flow rate of hydrogen as manipulated variable. The cell temperature is controlled by using the inlet flow rate of air as manipulated variable.

The control performance of the PI controller are investigated. Two PI control loops are adopted to control the PEMFC operation under the variation of current density as disturbance. The first loop is designed by using the first PI controller with the molar flow rate of air as manipulated variable to maintain the cell temperature whereas the second loop is designed by using another PI controller with the inlet flow rate of hydrogen as manipulated variable to regulate partial pressure of hydrogen. The simulation results revealed that the cell temperature raises a transient response up and backs to a steady state response since the inlet flow rate of air is adjusted under the disturbances. Moreover, the variation of the partial pressure of hydrogen decreases because the hydrogen consumption is high with increasing current density, hence the PI controller speeds up hydrogen flow rate in order to compensate the level of hydrogen consumption. Although the PI controller can be well designed for PEMFC system, it still has low robust ability and cannot deal with its high nonlinearity.

For the performance control of the MPC controller. The molar flow rate of air as manipulated variable to maintain the cell temperature whereas the inlet flow rate of hydrogen as manipulated variable to regulate partial pressure of hydrogen. The simulation results revealed that the MPC controller is able to track the set-point value when initial value of the cell temperature is equal to 10 K. Although there is a small oscillation in the regulated outputs, the cell temperature and partial pressure of hydrogen can reach the set-point value within 1,000 sec.

For the performance control of the robust MPC controller. In this work, one uncertain parameter as the cell voltage is randomly time-varying between 0.55 V and 0.65 V. The simulation results revealed that a robust MPC algorithm using ellipsoidal invariant can maintain the regulated outputs by manipulating the control inputs to their set-points. The cell voltage can track to the desire value. It means that also guarantee robust stability of a PEMFC system. Moreover, it can be observed that an off-line robust MPC algorithm using ellipsoidal invariant can achieve better control performance than a PI and MPC controller because an off-line robust MPC can guarantee robust stability.

6.2 Recommendations

1. A PEMFC is a multi-input-multi-output (MIMO) system. MIMO control problem is complex because there are many controlled and manipulated variables and process interaction among their variables. It may become poor performance control. Changes in manipulated variables impact to all of controlled variables, therefore control structure design and pairing of controlled and manipulated variable is important for PEMFC system.

2. For control design, this research concludes that an off-line robust MPC algorithm using ellipsoidal invariant is the best control performance because they can deal with uncertain parameter. But we considered a small number of vertices, therefore an off-line robust MPC algorithm should be considered by using polyhrdral invariant.

REFERENCES

Ahn, J.-W. and S.-Y. Choe (2008). "Coolant controls of a PEM fuel cell system." Journal of Power sources **179**(1): 252-264.

Alejandro, J., A. Arce, et al. (2007). "Development and experimental validation of a PEM fuel cell dynamic model." Journal of Power sources **173**(1): 310-324.

Amphlett, J., R. Mann, et al. (1996). "A model predicting transient responses of proton exchange membrane fuel cells." Journal of Power sources **61**(1): 183-188.

Araki, T., H. Koori, et al. (2005). "Simulation of the current density distribution for a PEMFC by using measured electrochemical and physical properties of the membrane." Journal of Power sources **152**: 60-66.

Arce, A., C. Panos, et al. (2011). Design and experimental validation of an explicit MPC controller for regulating temperature in PEM fuel cell systems. Proceedings of the 18th IFAC World Congress.

Baboli, M. K. and M. Kermani (2008). "A two-dimensional, transient, compressible isothermal and two-phase model for the air-side electrode of PEM fuel cells." Electrochimica Acta **53**(26): 7644-7654.

Bernardi, D. M. and M. W. Verbrugge (1992). "A mathematical model of the solid-polymer-electrolyte fuel cell." Journal of the Electrochemical Society **139**(9): 2477-2491.

Bordons, C., A. Arce, et al. (2006). Constrained predictive control strategies for PEM fuel cells. American Control Conference, 2006, IEEE.

Chang, S.-M. and H.-S. Chu (2006). "Transient behavior of a PEMFC." Journal of Power sources **161**(2): 1161-1168.

Chen, Q., L. Gao, et al. (2009). "Multiple model predictive control for a hybrid proton exchange membrane fuel cell system." Journal of Power sources **191**(2): 473-482.

Chiu, H.-C., J.-H. Jang, et al. (2012). "A three-dimensional modeling of transport phenomena of proton exchange membrane fuel cells with various flow fields." Applied Energy **96**: 359-370.

Feroldi, D. and M. Basualdo (2012). Description of PEM fuel cells system. PEM Fuel Cells with Bio-Ethanol Processor Systems, Springer**:** 49-72.

Gruber, J., C. Bordons, et al. (2012). "Nonlinear MPC for the airflow in a PEM fuel cell using a volterra series model." Control Engineering Practice **20**(2): 205-217.

Gruber, J., M. Doll, et al. (2009). "Design and experimental validation of a constrained MPC for the air feed of a fuel cell." Control Engineering Practice **17**(8): 874-885.

Gruber, J. K., C. Bordons, et al. (2008). Nonlinear control of the air feed of a fuel cell. American Control Conference, 2008, IEEE.

Hu, M., A. Gu, et al. (2004). "Three dimensional, two phase flow mathematical model for PEM fuel cell: Part I. Model development." Energy Conversion and Management **45**(11): 1861-1882.

Hu, P., G.-Y. Cao, et al. (2010). "Coolant circuit modeling and temperature fuzzy control of proton exchange membrane fuel cells." International Journal of Hydrogen Energy **35**(17): 9110-9123.

Jang, J.-H., W.-M. Yan, et al. (2006). "Effects of the gas diffusion-layer parameters on cell performance of PEM fuel cells." Journal of Power sources **161**(1): 323-332.

Ju, H., H. Meng, et al. (2005). "A single-phase, non-isothermal model for PEM fuel cells." International Journal of Heat and Mass Transfer **48**(7): 1303-1315.

Khan, M. and M. Iqbal (2005). "Modelling and Analysis of Electro-chemical, Thermal, and Reactant Flow Dynamics for a PEM Fuel Cell System." Fuel cells **5**(4): 463-475.

Kothare, M. V., V. Balakrishnan, et al. (1996). "Robust constrained model predictive control using linear matrix inequalities." Automatica **32**(10): 1361-1379.

Litster, S. and G. McLean (2004). "PEM fuel cell electrodes." Journal of Power sources **130**(1): 61-76.

Matamoros, L. and D. Brüggemann (2006). "Simulation of the water and heat management in proton exchange membrane fuel cells." Journal of Power sources **161**(1): 203-213.

Meidanshahi, V. and G. Karimi (2012). "Dynamic modeling, optimization and control of power density in a PEM fuel cell." Applied Energy **93**: 98-105.

Methekar, R., S. Patwardhan, et al. (2010). "Control of proton exchange membrane fuel cells using data driven state space models." Chemical Engineering Research and Design **88**(7): 861-874.

Methekar, R., V. Prasad, et al. (2007). "Dynamic analysis and linear control strategies for proton exchange membrane fuel cell using a distributed parameter model." Journal of Power sources **165**(1): 152-170.

Mueller, F., J. Brouwer, et al. (2007). "Quasi-three dimensional dynamic model of a proton exchange membrane fuel cell for system and controls development." Journal of Power sources **163**(2): 814-829.

Na, W. K. and B. Gou (2008). "Feedback-linearization-based nonlinear control for PEM fuel cells." Energy Conversion, IEEE Transactions on **23**(1): 179-190.

Niknezhadi, A., M. Allué-Fantova, et al. (2011). "Design and implementation of LQR/LQG strategies for oxygen stoichiometry control in PEM fuel cells based systems." Journal of Power sources **196**(9): 4277-4282.

Panos, C., K. Kouramas, et al. (2012). "Modelling and explicit model predictive control for PEM fuel cell systems." Chemical Engineering Science **67**(1): 15-25.

Pathapati, P., X. Xue, et al. (2005). "A new dynamic model for predicting transient phenomena in a PEM fuel cell system." Renewable energy **30**(1): 1-22.

Pukrushpan, J. T., A. G. Stefanopoulou, et al. (2002). Modeling and control for PEM fuel cell stack system. American Control Conference, 2002. Proceedings of the 2002, IEEE.

Rismanchi, B. and M. Akbari (2008). "Performance prediction of proton exchange membrane fuel cells using a three-dimensional model." International Journal of Hydrogen Energy **33**(1): 439-448.

Seborg, D. E., D. A. Mellichamp, et al. (2010). Process dynamics and control, John Wiley & Sons.

Shen, M., W. Meuleman, et al. (2003). "The characteristics of power generation of static state fuel cells." Journal of Power sources **115**(2): 203-209.

Skogestad, S. (2004). "Control structure design for complete chemical plants." Computers & Chemical Engineering **28**(1): 219-234.

Vahidi, A., A. Stefanopoulou, et al. (2006). "Current management in a hybrid fuel cell power system: A model-predictive control approach." Control Systems Technology, IEEE Transactions on **14**(6): 1047-1057.

Wu, W., J. Xu, et al. (2009). "Multi-loop nonlinear predictive control scheme for a simplistic hybrid energy system." International Journal of Hydrogen Energy **34**(9): 3953-3964.

Xue, X., J. Tang, et al. (2004). "System level lumped-parameter dynamic modeling of PEM fuel cell." Journal of Power sources **133**(2): 188-204.

Yerramalla, S., A. Davari, et al. (2003). "Modeling and simulation of the dynamic behavior of a polymer electrolyte membrane fuel cell." Journal of Power sources **124**(1): 104-113.

Zhao, Y. and E. Pistikopoulos (2013). "Dynamic modelling and parametric control for the polymer electrolyte membrane fuel cell system." Journal of Power sources **232**: 270-278.

Zhou, B., W. Huang, et al. (2006). "Water and pressure effects on a single PEM fuel cell." Journal of Power sources **155**(2): 190-202.

Ziogou, C., S. Papadopoulou, et al. (2013). "On-line nonlinear model predictive control of a PEM fuel cell system." Journal of Process Control **23**(4): 483-492.

APPENDIX

APPENDIX A

PROOF OF LINEAR OBJECTIVE MINIMIZATION PROBLEM

Let be $x(k) = x(k|k)$ the state of the uncertain system (A.1) measured at sampling time k.

$$\begin{aligned} x(k+1) &= A(k)x(k) + B(k)u(k) \\ y(k) &= Cx(k) \\ [A(k)\ B(k)] &\in \Omega \end{aligned} \tag{A.1}$$

To guarantee the robust stability to the closed-loop, the state feedback gain, F is proved to satisfy the lyapunov stability constraint.

Derivation of the upper bound, assume V satisfies the following inequality for all $x(k) = x(k+i|k), u(k+i|k), i \geq 0$ satisfying (A.1), and for any $[A(k)\ B(k)] \in \Omega, i \geq 0$. We get

$$V(x(k+i+1|k)) - V(x(k+i|k)) \leq -\left[x(k+i|k)^T \Theta\, x(k+i|k) + u(k+i|k)^T\, R\, u(k+i|k)\right] \tag{A.2}$$

Substituting

$$u(k+i|k) = Kx(k+i|k) \tag{A.3}$$

$$V(x(k|k)) = x(k|k)^T\, Px(k|k) \tag{A.4}$$

$$x(k+i+1|k) = (A(k+i) + B(k+i)K)x(k+i|k) \tag{A.5}$$

The quadratic function V required to satisfy becomes

$$\begin{aligned} &x(k+i+1|k)^T\, Px(k+i+1|k) - x(k+i|k)^T\, Px(k+i|k) \\ &\leq -\left[x(k+i|k)^T \Theta\, x(k+i|k) + Kx(k+i|k)^T\, R\, Kx(k+i|k)\right] \end{aligned} \tag{A.6}$$

$$\begin{aligned}&\left[A(k+i)+B(k+i)K\right)x(k+i|k)\right]^T P\left[A(k+i)+B(k+i)K\right)x(k+i|k)\right]\\&-x(k+i|k)^T Px(k+i|k)\le-\left[x(k+i|k)^T\left[\Theta+K^T RK\right]x(k+i|k)\right]\end{aligned}\tag{A.7}$$

$$\begin{aligned}&x(k+i|k)^T\left[(A(k+i)+B(k+i))^T P(A(k+i)+B(k+i)K)-P\right]x(k+i|k)\\&\le-\left[x(k+i|k)^T\left[\Theta+F^T RK\right]x(k+i|k)\right]\end{aligned}\tag{A.8}$$

$$x(k+i|k)^T\left[(A(k+i)+B(k+i)K)^T P(A(k+i)+B(k+i)K)-P+\Theta+K^T RK\right]x(k+i|k)\le 0\tag{A.9}$$

That is satisfied for all $i\ge 0$ if

$$\left[(A(k+i)+B(k+i)K)^T P(A(k+i)+B(k+i)K)-P+\Theta+K^T RK\right]\le 0\tag{A.10}$$

Substituting

$$P=\gamma Q^{-1}, Q>0\tag{A.11}$$

and

$$Y=KQ\tag{A.12}$$

Then pre- and post- multiplying by Q

$$\begin{aligned}&(A(k+i)Q+B(k+i)KQ)^T\gamma Q^{-1}(A(k+i)Q+B(k+i)KQ)\\&-Q\gamma Q^{-1}Q+Q\Theta Q+QK^T RKQ\le 0\end{aligned}\tag{A.13}$$

$$\begin{aligned}&(A(k+i)Q+B(k+i)Y)^T\gamma Q^{-1}(A(k+i)Q+B(k+i)Y)\\&-Q\gamma+Q\Theta Q+Y^TRY\le 0\end{aligned} \tag{A.14}$$

Convert to LMI form using Schur complements

$$\begin{bmatrix} Q & QA(k+i)^T+Y^TB(k+i)^T & Q\Theta_1^{1/2} & Y^TR^{1/2}\\ A(k+i)Q+B(k+i)Y & Q & 0 & 0\\ \Theta_1^{1/2}Q & 0 & \gamma I & 0\\ R^{1/2}Y & 0 & 0 & \gamma I \end{bmatrix} \tag{A.15}$$

Using Schur complement, let $Q(x)=Q(x)^T, R(x)=R(x)^T$, and $S(x)$ defined affinely on x. the matrix inequalities

$$Q(x)-S(x)R(x)^{-1}S(x)^T>0, R(x)>0 \tag{A.16}$$

or,

$$R(x)-S(x)^TQ(x)^{-1}S(x)>0, Q(x)>0 \tag{A.17}$$

is equivalent to the linear matrix inequalities (LMIs)

$$\begin{bmatrix} Q(x) & S(x)\\ S(x)^T & R(x)\end{bmatrix}>0 \tag{A.18}$$

VITA

Miss Thanaphorn Hakhen was born on December 25th, 1988 in Udornthani, Thailand. She finished high school from Udonpittanukoon School, Udornthani. She received the Bachelor's Degree in Chemical Engineering from King Mongkut's University of Technology Thonburi in 2010. She subsequently continued studying the Master of Engineering in Chemical Engineering at the Graduate School of Chulalongkorn University (Chulalongkorn University scholarship). She has been studying Master's Degree of Chemical Engineer in 2014